

**Design of single effect solar powered absorption  
Air-conditioning system with ammonia-water working fluid**

Thesis submitted in partial fulfilment of the requirement for the degree of Master  
of Power Engineering from the Faculty of Engineering & Technology of Jadavpur  
University in the year of 2016-17

Submitted By

Srabanti Ghosh

Examination Roll No: M4POW1616

Registration No: 125000 of 13-14

Under the guidance of

Prof. Amitava Datta

Department of Power Engineering

Jadavpur University

Salt Lake Campus

Kolkata - 700098

**Jadavpur University**  
**Faculty of Engineering & Technology**

Certificate of Recommendation

I hereby recommend that the thesis entitled as “**Design of Single Effect Solar Powered Absorption Air-Conditioning System With Ammonia-Water Working Fluid**” prepared by **Srabanti Ghosh** (Regn.No 125000 of 2013-14) under my guidance, be accepted in a partial fulfillment of the requirement for the degree of **Master of Power Engineering** from the department of Power engineering of Jadavpur University.

---

(THESIS ADVISOR)

COUNTERSIGNED

---

(HEAD OF THE DEPARTMENT)

---

(DEAN OF FACULTY OF ENGG. & TECH.)

JADAVPUR UNIVERSITY

**Jadavpur University****Faculty of Engineering & Technology**Certificate of Approval

The foregoing thesis, entitled as “**Design of Single Effect Solar Powered Absorption Air-Conditioning System with Ammonia-Water Working Fluid**”, is hereby approved by the committee of final examination for evaluation of thesis as a creditable study of an engineering subject carried out and presented by **Srabanti Ghosh** (Regn. No. 125000 of 2013-14) in a manner satisfactory to warrant its acceptance as a requisite to the degree of **Master of Power Engineering**. It is understood that by this approval, the undersigned do not necessarily endorse or approve any statement made, opinion expressed or conclusion drawn therein, but approve the thesis only for the purpose for which it is submitted.

COMMITTEE OF FINAL EXAMINATION FOR

EVALUATION OF THESIS

---

(EXTERNAL EXAMINER)

---

(THESIS ADVISOR)

## **Declaration of Originality and Compliance of Academic Ethics**

I hereby declare that this thesis entitled “Design of Single Effect Solar Powered Absorption Air-Conditioning System with Ammonia-Water Working Fluid” contains literature survey and original research work by the undersigned candidate, as part of Degree of Master of Engineering in Power Engineering studies.

All information in this document has been obtained and presented in accordance with academic rules and ethical conduct.

I also declare that, as required by these rules and conduct, I have fully cited and referenced all material and results that are not original to this work.

Name (Block Letters): SRABANTI GHOSH

Examination Roll Number: M4POW1616

Registration No: 125000 of 2013-14

Class Roll No: 001311502005

Signature with Date:

## Acknowledgement

The author remembers with gratitude the constant guidance, suggestions, encouragement and support forwarded by several respected persons and knows well that it is not possible to express her humility for all those valuable assistances in this finite piece of paper. Following conventions, she therefore, acknowledges here the assistance rendered by each and every person, as a token of thanks.

The author thankfully acknowledges the kind and persistent valuable suggestion, advice, guidance, help and encouragement from Prof. Amitava Datta without which this thesis would not have been completed.

The author likes to convey her gratitude to the faculty in M.E. course of Power Engineering department of Jadavpur University for the excellent teaching that has helped a lot to complete the project smoothly.

The author thanks all her co workers, Mr. Mithun Das, Mr. Pritam Kumar Das, Mr. Atmadeep Bhattacharya and Mr. Abhirup Ghosh both in the same laboratory and from other laboratories of the department for the valuable time they have spared giving ideas and suggestions wherever and whenever necessary.

Last but not the least the author conveys her humility and gratitude to God, family and friends who have always been a constant inspiration source in each and every work that finally contributed to the successful completion of this work.

**Srabanti Ghosh**

## Abstract

In this study, a solar powered single stage absorption air-conditioning system, using ammonia-water solution is designed by numerical programming method using MATLAB 8.1. The main components of such system are: solar collector, storage tank, solution pump and absorption cooling system. 10 numbers of 2 ton air-conditioning system i.e. about 70 KW cooling load is taken. To drive this 70 KW cooling load for Kolkata, India the required solar collector area is 372 m<sup>2</sup>. This 372 m<sup>2</sup> collector area fulfilled the system requirement when the operating load is 10 hour a day in summer and 8 hour a day in winter. A modular software programme is developed to evaluate the coefficient of performance of the absorption air-conditioning system by varying the various parametric conditions  $T_g = 60^\circ\text{C to } 90^\circ\text{C}$ ,  $T_c = 20^\circ\text{C to } 40^\circ\text{C}$ ,  $T_e = -5^\circ\text{C to } 7.5^\circ\text{C}$ ,  $T_a = 20^\circ\text{C to } 40^\circ\text{C}$ . Among this most optimum value of COP is selected to operate the cooling load. The optimum condition at which the air-conditioning load is operate is  $T_g = 90^\circ\text{C}$ ,  $T_c = 20^\circ\text{C}$ ,  $T_e = 7.5^\circ\text{C}$ ,  $T_a = 25^\circ\text{C}$ . The effect of various component temperatures on coefficient of performance has been studied. Also the hourly variation of storage tank temperature is investigated in details and it is shown how the storage tank fulfill its purpose by taking care of the approximate mismatching between useful heat and load demand of the system.

## **Nomenclature**

$\dot{m}$  = Mass flow rate (Kg/minutes)

$T_g$  = Generator temperature (K)

$T_c$  = Condenser temperature (K)

$T_e$  = Evaporator temperature (K)

$T_a$  = Absorber temperature (K)

P = pressure (Kpa)

X = Mass fraction of ammonia in liquid phase (decimal)

$\bar{X}$  = Mole fraction of ammonia in liquid phase (decimal)

Y = Mass fraction of ammonia in vapor phase (decimal)

$\bar{Y}$  = Mole fraction of ammonia in vapor phase (decimal)

$C_p$  = Specific thermal capacity (KJ/mol K)

$T_c$  = Critical temperature

$h$  = Enthalpy (KJ/Kg)

$\dot{Q}$  = Heat transfer rate (KW)

COP = Coefficient of performance

E = Solar irradiance

n = Number of days

r = Titled factor

A = Area (m<sup>2</sup>)

Q = Thermal energy

## **Greek Symbols**

$\theta$  = Solar zenith angle

$\gamma$  = Solar azimuth angle

$\beta$  = Solar tilted angle

$\varphi$  = Latitude

$\rho$  = Ground reflectivity

$\epsilon$  = collector efficiency

$\tau$  = Transmittivity

$\alpha$  = Absorptivity

### **Subscript**

a = Absorber

c = Condenser

e = Evaporator

g = Generator

h = High

l = Low

sat = Saturate

sol = Solution

p = pump

ss = Strong solution

ws = Weak solution



**List of Figures****Page No.**

Figure 1: Growth in total primary energy demand from 1987-2035	15
Figure 2: Worldwide energy intensity from 1970-2030	16
Figure 3: Resource wise future consumption of energy up to 2035	17
Figure 4: Global primary energy consumption by 2050	18
Figure 5: Change in population (in million) without access of electricity from 2010 to 2050	20
Figure 6: Source wise total global energy consumption	22
Figure 7: Sector wise total global energy consumption	22
Figure 8: Sector wise total energy consumption in India	23
Figure 9: Energy consumption in India resource wise	23
Figure 10: Cumulative electricity and natural gas bill saving by sector in (billion)	28
Figure 11: Global new investment in renewable energy by source in 2014 and growth on 2013 in billion \$	30
Figure 12: Global investment in renewable energy by asset class, 2004-2014	31
Figure 13: Vapor compression refrigeration cycle	34
Figure 14: Absorption refrigeration cycle	35
Figure 15: classification of solar collector	41
Figure 16: Schematic diagram of Evacuated tube solar collector	42
Figure 17: Schematic diagram of solar absorption refrigeration system	51
Figure 18 (a): Variation of coefficient of performance with generator temperature	62
Figure 18 (b): Variation of circulation ratio with generator temperature	63
Figure 19: Variation of mass fraction with temperature	63

---

Figure 20 (a): Variation of coefficient of performance with absorber temperature	64
Figure 20 (b): Variation of circulation ratio with absorber temperature	65
Figure 21: Variation of coefficient of performance with condenser temperature	66
Figure 22: Variation of coefficient of performance with evaporator temperature	67
Figure 23: Hourly variation of storage tank temperature for summer month	68
Figure 24: Hourly variation of storage tank temperature for winter month	68

**List of tables****Page No**

Table 1: The energy demand in Terawatt hour changes from 2005 to 2020	21
Table 2: The share of different renewable energy resources in India from 2012-2022	22
Table 3: The various energy resources with their respective installed capacity ( in MW) In India as per the data on 28-feb-2015	24
Table 4: Installed capacity of renewable energy resources in India	25
Table 5: different working fluid used in absorption refrigeration system	39

**CONTENT****Page No****CHAPTER 1****Introduction**

1.1 Present energy scenario	14
1.1.1 World energy scenario	14
1.1.2 World energy consumption	15
1.1.3 Variation of energy intensity region-wise	16
1.1.4 Investment in renewable resource and recent development	16
1.1.5 Future consumption of energy by fuel	17
1.1.6 The primary energy supply by different region	18
1.1.7 Future investment need in electricity generation	19
1.1.8 Access to electricity	19
1.1.9 Energy scenario in India	20
1.1.10 Total global energy consumption	22
1.1.11 Total energy consumption in India	23
1.1.12 Objective of using renewable resources	25
1.1.13 Status of clean energy development	29
1.2 Importance of solar energy in the present context	31
1.3 Refrigeration cycle	33
1.3.1 Vapor-compression refrigeration cycle	33
1.3.2 Vapor-absorption refrigeration cycle	35
1.3.3 Advantage of vapor-absorption refrigeration cycle	37
1.3.4 Limitation of vapor-absorption refrigeration cycle	38
1.3.5 Different working fluid used in absorption refrigeration cycle	39
1.3.6 Collection of solar energy and classification of solar collector	40
1.3.7 Reason of using evacuated tube solar collector	41
1.3.8 Evacuated tube solar collector	42
1.4 Literature review	43
1.4.1 State of art for absorption refrigeration system	43
1.4.2 State of art for solar driven absorption cooling system	45
1.4.3 State of art for solar driven air-conditioning system	46
1.5 Scope of present work	48

## **CHAPTER 2**

### **Methodology**

2.1	Description of the system	50
2.2	Mathematical modeling	52

## **CHAPTER 3**

### **Result & Discussion**

3.1	Performance evaluation of absorption refrigeration system under different parametric condition	62
3.1.1	Effect of generator temperature	62
3.1.2	Effect of absorber temperature	64
3.1.3	Effect of condenser temperature	66
3.1.4	Effect of evaporator temperature	67
3.2	Design calculation of solar powered vapor absorption air-conditioning system	68

## **CHAPTER 3**

### **Conclusion and scope of future work**

4.1	Conclusion	72
4.2	Scope of future work	73
	Appendix	74
	Reference	79

## **CHAPTER 1**

### **Introduction**

**Present energy scenario**

**Importance of solar energy in the present context**

**Refrigeration cycle**

**Literature review**

**Scope of present work**

## Introduction

### 1.1 PRESENT ENERGY SCENARIO

Energy scenario provides a framework for exploring future energy perspective including various combinations of technology options and their implications. Energy scenario illustrates how the developments in the energy sector affect the global issues, like economic development, rise in human development index, sustainability etc. It describe how the future energy use will be compatible with the sustainable development and availability of energy resources. Energy scenario also gives a clear picture on the relationship between future energy consumption and economic growth or increased GDP [1].

#### 1.1.1 World energy scenario

According to World Energy Council (WEC), future energy scenario drives the world towards a specific objective such that we can think of different alternative options in case of uncertainties. It is well known that the increase in energy consumption is totally dependent on the population and income growth. By 2030 world population is projected to reach 8.3 billion, which means an additional 1.3 billion people will require energy for their use. On the other hand, the world income in 2030 is expected to be roughly double of that in 2011 in real terms [2].

The use of energy can be divided sector-wise as industrial, commercial, domestic, transportation and agricultural and other sectors. The population growth in the developing countries, due to rapid urbanization, is expected to increase the energy use in the domestic sector by nearly 90% within 2030. However, the growth in the primary energy demand is mainly led by the industrial sector. It has been noticed from every future projection that countries like India, China will dominate the energy production growth in future, both due to their large population and rapid economic development. Energy price also plays a key role for changing the response of the global energy system.

Improvement in energy-efficient devices and introduction of energy management practices are key factors to meet the global energy challenge. Higher efficiency of the equipment helps to reduce the energy loss at the devices and therefore the per capita energy requirement also reduced. Proper energy management identifies process flow path with reduced energy spillage. One practice in the energy management can be proper utilization of the energy resources. During the present time, thrust has been increased for the use of renewable resources to overcome the problem of depletion of conventional fossil fuel.

### 1.1.2 World Energy Consumption

World energy consumption refers to the total energy used by all the human civilization. It is evident from the (Fig.1) that fossil fuels remain the dominant source of energy powering the global economy for the period 1987-2011. For this period primary energy consumption is maximum for coal compared to natural gas and oil. For the period 2011-2035 the consumption is maximum for natural gas. It is shown from the below figure that the consumption of renewable energy is much higher during the year 2011- 2035 compare to the period 1987-2011.

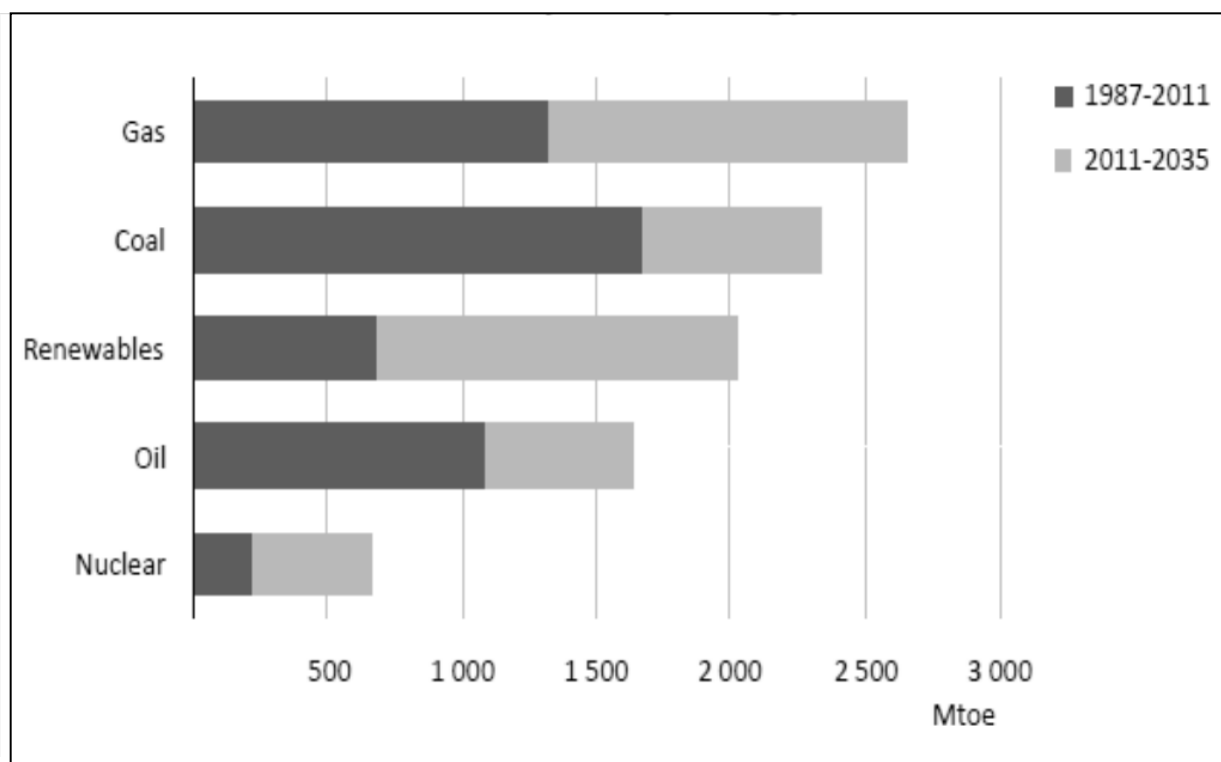
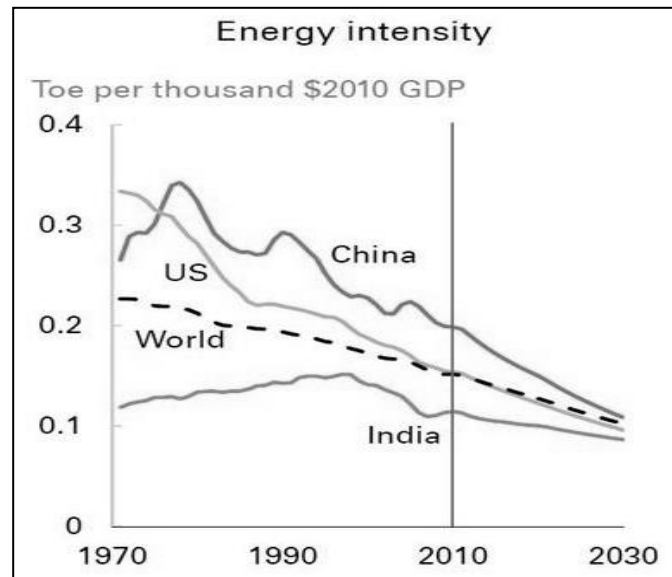


Figure 1: Growth in total primary energy demand from 1987-2035 [3]



### 1.1.3 Variation of energy intensity region-wise:



**Figure 2: Worldwide energy intensity from 1970-2030 [3]**

From (Fig.2) we have seen the declining and converging trend of energy intensity (the amount of energy consumption per unit of GDP) with respect to the years from 1970-2030. Current high price of energy and global integration reinforce this trend. Global energy intensity in 2030 is 31% lower than in 2011, declining at 1.9 % p.a compared to declining rate of 1.0 % p.a for 2000-10. It is evident from (Fig.2) that in case of India energy intensity increase up to 2000 and then starts to decline up to 2030 [2].

### 1.1.4 Investment in renewable resources and recent development

Due to increase in energy demand, high investment is always required not only for the consumption of conventional resources, but also for the new technologies use for harnessing the alternative energy resources. The “Shale revolution”, related to the tremendous production of oil and natural gas by using advance technology i.e. a new combination of horizontal drilling and hydraulic fracturing is the example of providing new technologies in harnessing energy resources in U.S.A. Renewable energy is one type of non fossil energy. We can get this type of energy by applying high efficiency technology.

But now a day’s application of renewable energy resources has been increased to reduce carbon emission because carbon emission reduction is a vital criterion for the world energy scenario. The share of renewable in primary energy use in the New Policies Scenario will rise to 18% in 2035, from 13% in 2011, resulting from rapidly increasing demand for modern renewable to generate power [3]. Power

Generation from renewable resources is increased by 7000 TWh from 2011 to 2035[3]. Renewable become the second largest source of electricity before 2015 and approach coal as the primary source by 2035.

Consumption of bio fuel is another renewable source of energy which is used as a transport fuel in recent decade. Consumption of bio fuels increase from 1.3mboe/d in 2011 to 4.1mboe/d in 2035, to meet 8% of fuel demand in road transport in 2035. The United States, Brazil, European Union and China meet more than 80% of all bio fuels demand [3]. So there is huge investment in this sector must be required to meet the energy demand along with reducing  $\text{CO}_2$  emission, reduction of other pollutant, lowering fossils-fuel import bill and charged up economic development.

### 1.1.5 Resource wise future energy consumption by Fuel

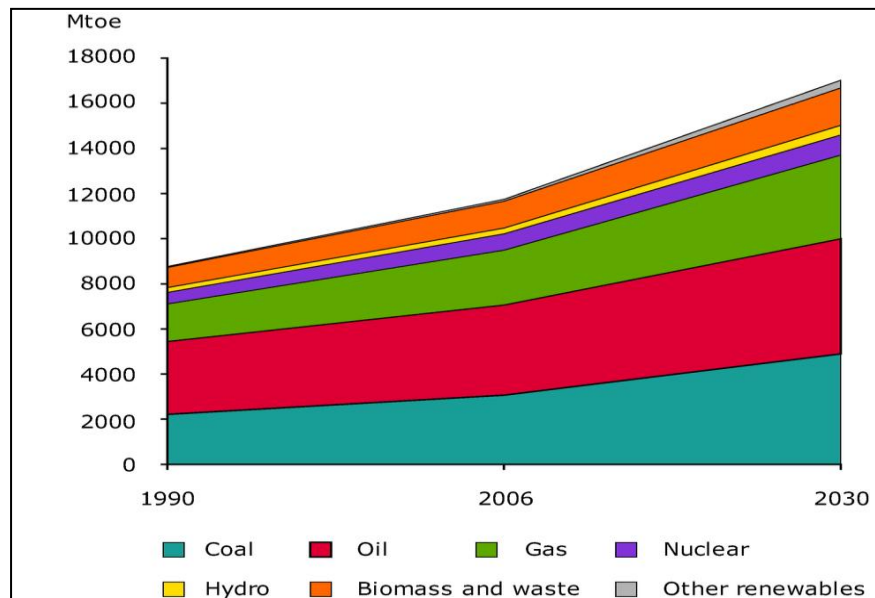


**Figure 3: Resource wise future consumption of energy up to 2030 [4]**

Figure.3 shows a strong growth for primary energy resources from 1990-2030. It is about 3000 Mtoe for coal, 3500 Mtoe for oil and 2000 Mtoe for natural gas. Consumption of renewable energy increases from 1990 to 2030. The BP Report shows strong growth in renewable energy, but it will be only about 8% of total global energy supply by 2030 [5].

### 1.1.6 The primary energy consumption by different region

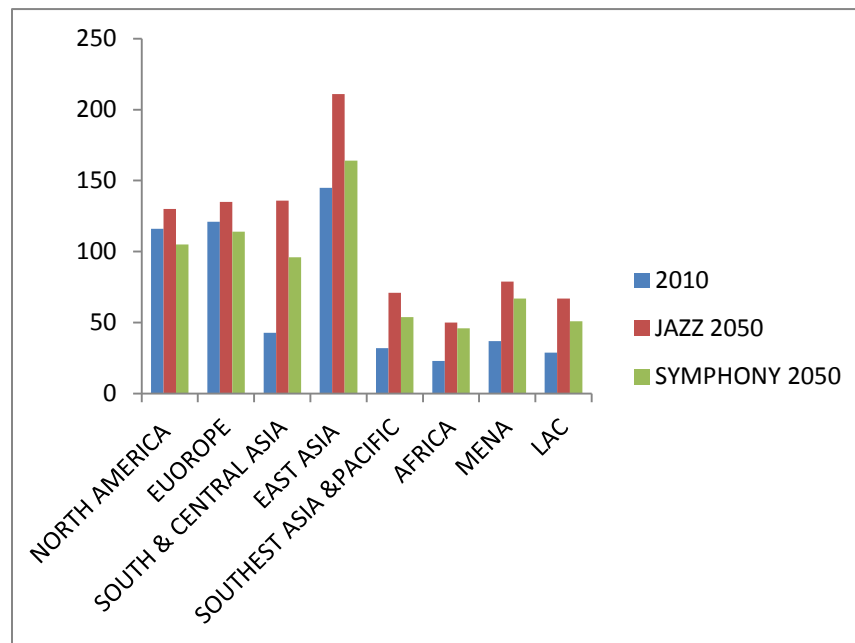


**Figure 4: Global primary energy consumption by 2050[1]**

WEC present two types of energy scenario up to 2050. These are Jazz and symphony.

- As an energy scenario JAZZ focus energy equity with priority given to achieving individual access and affordability of energy through economic growth and
- According to symphony it focuses on achieving sustainable development through internationally co-ordinated policies and practices.

Due to this ever increasing economical growth it is quite difficult to meet such energy demand. The WEC has estimated that total primary energy consumption will increase globally from 546EJ (100 Pwh) in 2010 to 849 EJ (184 Pwh) in JAZZ scenario and 696EJ (155 Pwh) in symphony scenario [1]. This corresponds to the increase in 61% in JAZZ and 27% in symphony. To meet both the global and regional energy demand is a challenge. Fig. 4 shows the global primary energy consumption up to the year 2050 for both the scenario with respect to 2010. It is evident from the Fig. 4 that the region wise energy consumption is higher in case of Jazz scenario compares to symphony scenario with respect to 2010 and the energy consumption is highest for East Asia.

The energy intensity according to both the scenarios changes to 4.4 and 4.1 in 2050 from 8.8 in 2010. The future energy mix in 2050 shows that growth rate will be highest for renewable energy sources.

In absolute term fossil fuel will dominant up to 2050. The share of fossil fuel will be 77% in JAZZ and 59% in symphony compare to 79 % in 2010. The use of renewable resources will increase from 15 % in 2010 to almost 30% in 2050. To meet the future energy demand and to maintain the compatibility with ever increasing economical growth rate the electricity generation have to increase from 21.5 billion MWH to 53.6 billion MWH i.e. about 150% [1].

### **1.1.7 Future investment need in electricity generation:**

The inflation adjusted price in the electricity market across the OECD countries increased by 2.8 % in households and 5.3% in industrial user between 2006 and 2013. Between now and 2040 electricity price will increase by 57% in EU and 50% in US due to the higher operational, maintenance, investment cost. About \$3 trillion has been already invested between 2000 and 2012 and an additional \$7.6 trillion require to be invested in the near future 2040. This high level investment will need to continue if the energy policy needs to be met. Investment needs in conventional, renewable, centralized, decentralized will be \$180 billion annually and in expansion, modernization, installation of transmission and distribution grid will be \$100 billion per year [6].

### **1.1.8 Growth of population access to electricity**

The degree of electrification measure in terms of the share of electrical energy will increase significantly up to 2050 is about 30 % in case of both the scenario compare to 17 % in 2010. In 2010 1.267 billion people were without access of electricity, this reduces to 319 million in jazz and 530 million in symphony scenario [7]. Population of without access of electricity is highest for sub-Saharan Africa followed by Fig.5. It is evident from Fig.5 that in East Asia number of people without access of electricity are very much lower, almost negligible.

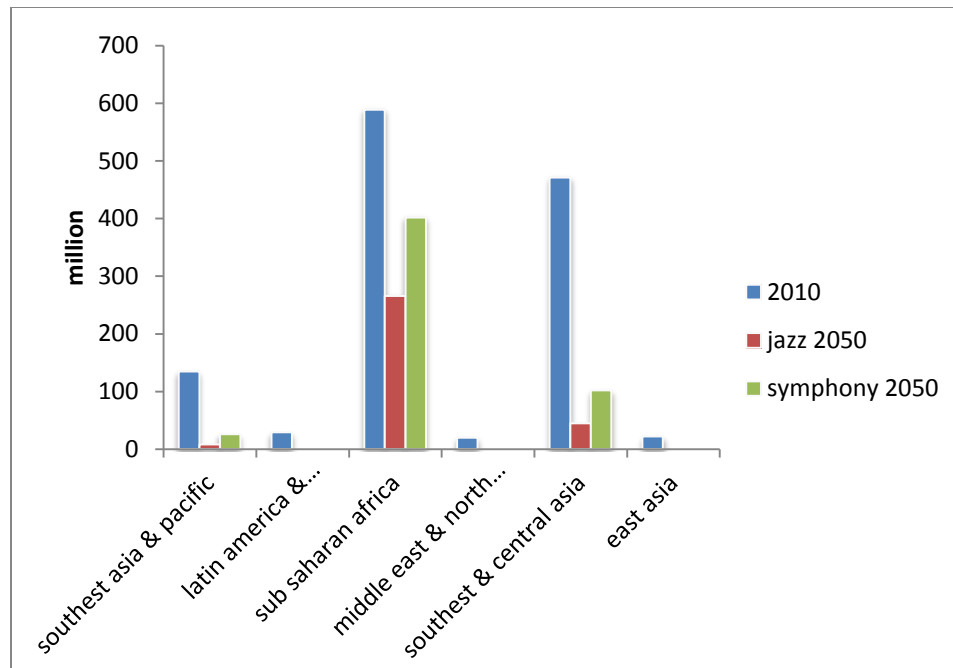


**Figure 5: Change in population (in million) without access of electricity from 2010 to 2050 [1]:**

### 1.1.9 National energy scenario

India is a country with more than 1.2 billion people accounting for more than 17% of world's population. It is the seventh largest country in the world. India has 29 states and 7 union territories. It faces a formidable challenge in providing energy to the users at a reasonable cost. It is anticipated that India's nominal GDP will exceed US \$ 3.5 trillion by March 2018. India's nominal GDP crossed the US \$ 1 trillion in 2007-2008 which means that the annual growth rate of nominal GDP during the period is very high, about 18 percent. Thus the energy challenge faced by the country is of fundamental importance. In the last six decades, energy use in India has increased by 16 times and the installed electricity capacity has increased by 84 times. In 2008, India acquires the fifth rank in the world in terms of energy use. Nevertheless, India as a country suffers from significant energy deficiency. In recent years, India's energy consumption has been increasing at a fast rate due to population growth and rapid economic development [8]. In this context sector wise energy demand in India from 2012 to 2047 has been listed in (table.1). It is seen from (table.1) that the energy demand is highest for industrial sector according to both the scenario, about 11,326 Terawatt for least effort scenario and 7960 Terawatt for heroic effort scenario with respect to baseline (2012) 2,278 Terawatt.

**Table 1: The energy demand in Terawatt hour changes from 2012 to 2047 [9]**

sector	Base line 2012	'Least effort' scenario 2047	'Heroic effort scenario' 2047
Commercial lighting & appliances	69.8	970.6	761.6
industry	2,278.80	11,326.40	7960.70
Rail transport	40.5	128.8	125.8
transport	847.9	6085.30	3035.00
agriculture	237.2	1047.80	533.1
House hold cooking	1,153.70	1069.20	616
cooking	1218.50	1808.20	1296.50
Gas service	449	769	2115

India is struggling with skyrocketing energy demand, declining energy supply and peak load blackout and shortage which limit the energy access.

Harnessing clean and renewable energy is the only solution to meet the ever increasing energy demands by sustainable way. In this scenario the growth in solar and wind power is remarkable.

In 2010, to meet the urgent and growing demand of energy by advancing clean energy solutions, the Government of India launched Jawaharlal Nehru National Solar Mission (NSM or Mission) to promote grid-connected and off-grid connected solar energy. The goal is to establish India as a global leader in solar energy through policies that lead to the deployment of 20 gig watts (GW) of solar power by 2022. The growth is remarkable i.e. from 20-30 MW/sq Km to 20,000 MW /sq Km followed by table.2. Solar photovoltaic (PV) power's installation capacity increased by 17.8 megawatts (MW) in early 2010 to approximately 2,650 MW in March 2014.

The Indian government accepts that wind energy can be a significant clean energy resource. It is seen from the (table. 2) that the share of renewable energy will be highest for wind power in the year 2022 i.e. in the 13<sup>th</sup> projected plan. Supported by initial government policies, India is the fifth-largest wind energy producer, achieving 20 Giga watts (GW) of installed capacity of wind power. Yet, much more have to be achieved. India has to increase its wind energy production about four to five times from its current level to achieve the country's 100 GW wind energy potential. To achieve the higher potential, the government announced plans in 2014 to launch a National Wind Energy Mission [10].

**Table 2: The share of different renewable energy resources in India from 2012 to 2022 [11 ]**

Resources	Potential (MW)	Up to 9 <sup>th</sup> plan	Up to 10 <sup>th</sup> plan	11 <sup>th</sup> plan target	Up to 30.09.2010	Cumulative achievement	12th plan projected (2017)	13 <sup>th</sup> plan projected (2022)
Wind power	48,500	1667	5427	9000	4714	12,809	27,300	38,500
Small hydro power	15,000	1436	538	1400	759	2823	5000	6,600
Bio power	23,700	390	795	1780	1079	2505	5700	7,300
Solar power	20-30 MW/sq km	2	1	50	8	18	4000	20,000
total		3497	6761	12,230	6560	18,155	41,400	72,400

### 1.1.10 The total global energy consumption

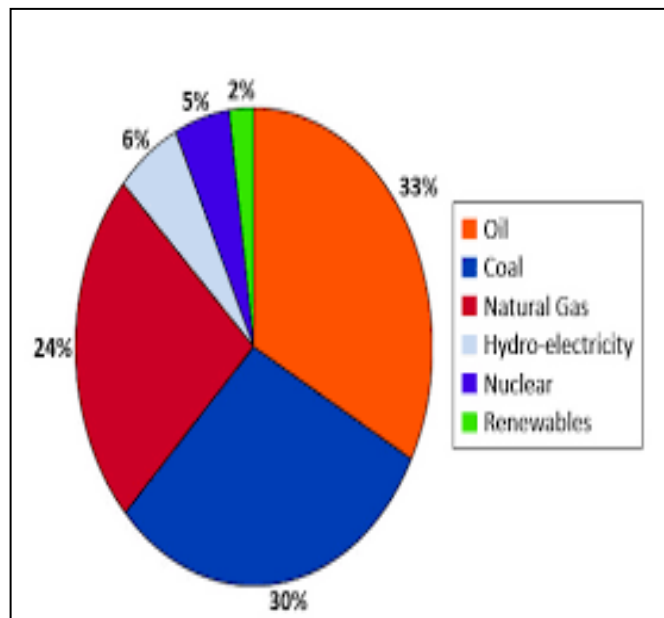


**Figure 6: Total global energy consumption (source wise) [12]**

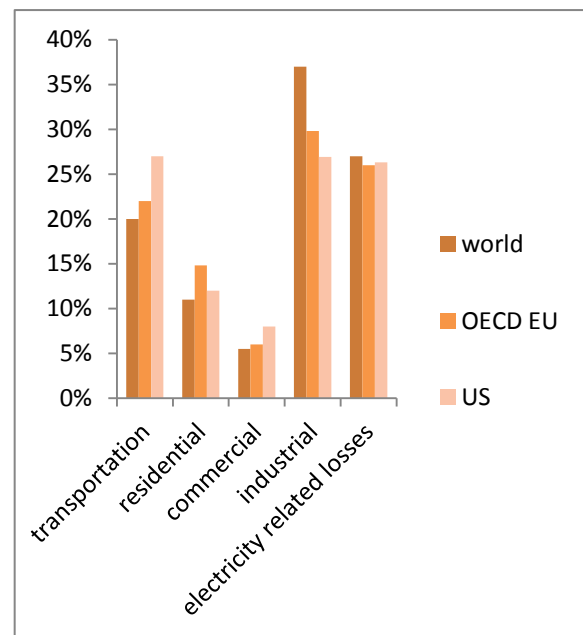


**Figure 7: Total global energy consumption (sector wise) [1]**

Figure.6 represents the total global energy consumption in resource wise. It is seen from Fig. (6) that total global energy consumption is highest for petroleum oil about 33% then coal about 30 % then

natural gas about 24 %. Global energy consumption for renewable resources is about 2 %. Figure.7 shows the sector wise global energy consumption and it is highest for industrial sector both for the world and OECD countries. Also the transportation sector shows the remarkable consumption of energy. Industrial sector consume about 38 % of total global energy and transportation sector consume about 27 % of total global energy in case of world.

### 1.1.11 The total energy consumption in India

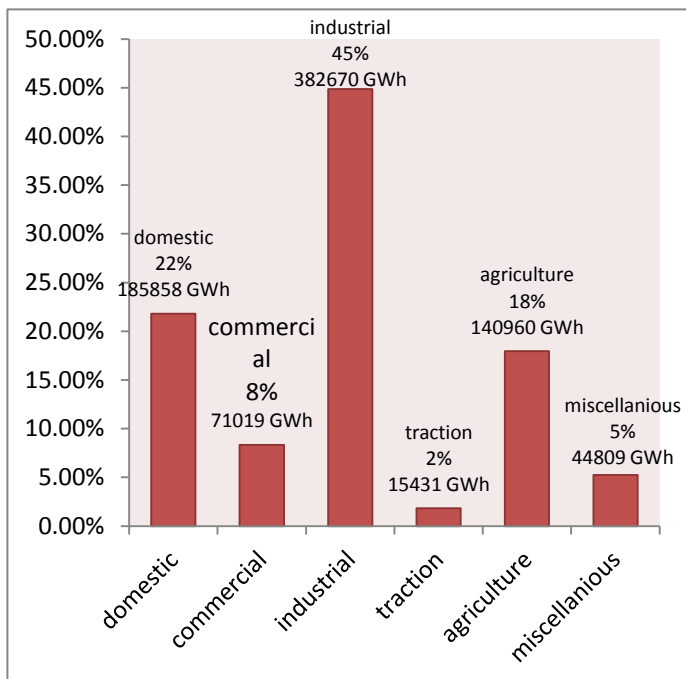


**Figure 8: Sector wise total energy consumption in India [13]**

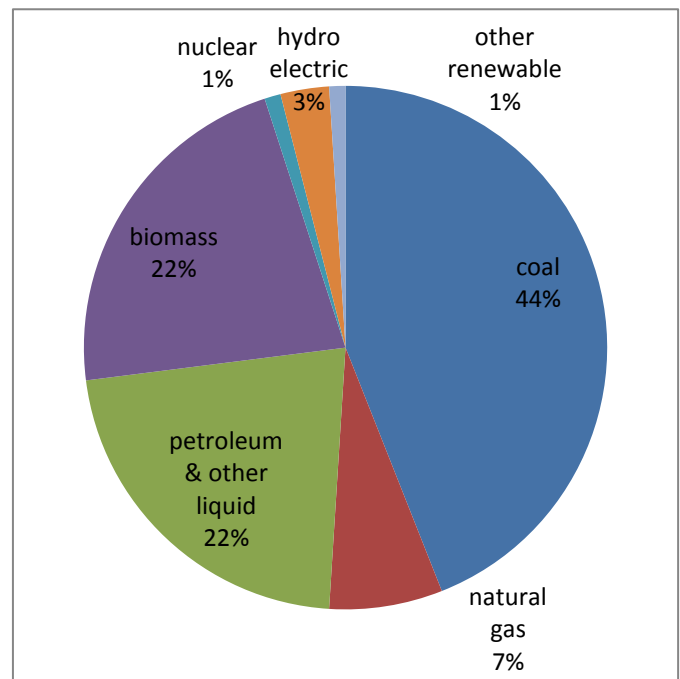


**Figure 9: Energy consumption in India Resource wise [14]**

The total installed electricity capacity in India is about 261.006 GW as on the end of February, 2015 and generated energy is about 966.777 BU from April, 2014 to February, 2015. India becomes the third largest country in terms of generation of electricity with 4.8 % global share of electricity by surpassing Japan and Russia. The total energy consumption in India is highest for industrial sector about 3, 82,670 Gwh (45 % of all sector) followed by Fig. 8. In India domestic sector also show remarkable consumption of energy about 1, 85,858 Gwh (20 % of total energy consumption). By analyzing fig. 9 we can say that the energy consumption is highest for coal in India, about 44 %. Petroleum and biomass



show the same amount of consumption i.e. 22 %. Natural gas shows the remarkably low consumption, about 7% compare to the global consumption about 24 %.

Renewable power plants constitute 27.80% of total installed capacity and non renewable consist of 72.20%. It is evident from (table.3) that as per the year 2015 the installed capacity is highest for coal about 158,496 MW i.e. 60.72 % of total installed capacity. The installed capacity for renewable energy is 72,491 MW i.e. about 28 % of total installed capacity.

**Table 3: The various energy resources with their respective installed capacity (in MW) in India as per the data on 28-feb-2015 as follows [15]**

<i>resources</i>	<i>Installed capacity in MW</i>
coal	158,496
Gas	22,971
diesel	1200
Sub-total thermal	182,667
nuclear	5780
Hydro	40,867
Other renewable	31,692
Subtotal renewable	72,491
Total power	261,006

India's electricity sector is the most active player in renewable energy utilization, specially the wind energy. As on 31<sup>st</sup> January 2014 India's total installed capacity was 31.15 GW only for non-conventional renewable technology based electricity. In this context the various renewable energy resources in India and their installed capacity are shown in (table.4). The installed capacity for wind power is highest in Gujarat, about 10,600 MW. Among all, the installed capacity is highest for hydro power about 33,774 MW i.e. 56 % of total grid connected installed capacity. For off grid connected power the installed capacity is highest for biogas cogeneration. Also solar photo voltaic show a remarkable installed capacity about 159 MW i.e. 16 % of total off grid connected installed capacity.

**Table 4: Installed capacity of renewable energy resources in India [16]**

Type	technology	Installed capacity(MW)	Type	technology	Installed capacity(MW)
<b>Grid connected power</b>	Wind	20,298.83 (Gujarat highest 10,600 MW)	<b>Off grid connected power</b>	Biogases Cogeneration	517.34
	Small hydro	33774.15		SPV system	159.77
	Bagasse cogeneration	2512.88		Biomass gasified-industrial	146.40
	solar	2208.36		Waste to power	119.63
	Biomass power gasification	1285.60		Biomass gasified-rural	17.63
	Waste to power	99.08		Water mill / micro hydro	20.18
			Aero generator hybrid system	2.18	
	Total	60,151.90		Total	983.13

### 1.1.12 Objective of using clean energy resources

The use of the conventional energy resources is making unfriendly impact on the environment. The burning of fossil fuel such as coal, oil, natural gas for generating electricity releases greenhouse gases and other pollutants into the atmosphere and results in the following impact to the earth and mankind:

#### **Global warming**

The greenhouse gases accelerate the insulating effect in the upper atmosphere preventing heat dissipation at the usual rate and results in global warming. The effect of global warming has far reaching impact on our ecosystem affecting the agricultural production and causing rise in the sea level.

#### **Atmospheric pollutant production**

Atmospheric pollutant such as sulphur-di-oxide, nitrogen oxide, respiratory suspended particulate etc affect the human health , with particular adverse effects on the young children and the aged as well as on the people with chronic health problem.

## **Economic development hindrance**

The reserve of fossil fuels is limited. Over the past decades, we have rapidly depleted these limited natural resources. As a result, the shortage of fossil fuel in the near future could adversely affect the activities of all walk of the life and hinder economic development. This could result in the global degradation of people's living standard.

The only solution to this problem is the clean energy:

Clean energy includes demand- and supply-side resources that meet energy demand with less pollution than that created by conventional, fossil-based generation. Clean energy technologies include:

**Increase in Energy efficiency (EE):** Energy efficiency means using less energy to provide the same or improved level of service to the consumer in an economically efficient way. Energy efficiency measures a wide variety of technologies and processes, can be implemented across all major energy-consuming sectors, and may affect all energy resources (e.g., natural gas, electricity, etc). Basically energy efficiency is a way of managing and restraining the growth in energy consumption. Devices are said to be energy efficient if it delivers more services for the same energy input, or the same services for less energy input. For example, when a compact florescent light (CFL) bulb uses less energy (one-third to one-fifth) than an incandescent bulb to produce the same amount of light, the CFL is considered to be more energy efficient.

**Use of Renewable energy (RE):** Renewable energy is the energy generated partially or entirely from non-depleting energy resources for direct end use or electricity generation. Renewable energy definitions vary by region, but usually include wind, solar, and geothermal energy. Some region also consider low-impact or small hydro, biomass, biogas, and waste-to-energy as a renewable energy resources. Renewable energy can be generated on site or at a central station.

**Introduction of Combined heat and power (CHP):** Combined heat and power (CHP) technology also known as cogeneration. CHP is a clean and efficient technology that improves the conversion efficiency of traditional energy systems by using waste heat from thermal power plant for heating or cooling in commercial or industrial facilities. CHP systems typically achieve 60% to 80% efficiencies, which is significantly higher than those of conventional power plants and separate steam units

**Clean distributed generation (DG):** Clean distributed generation refers to small-scale renewable energy and CHP at the customer or end-use site [17].

Clean energy resources — wind, solar, geothermal, hydroelectric, and biomass — provide substantial benefits for the climate, health, and economy. These benefits are as follows:

**Little to No Global Warming:** Human activities are overstressing the atmosphere by emitting carbon-di-oxide and other green house gases. These green house gases trap heat and drives up the surface temperature of earth causing harmful effects on our health, environment and climate.

About one third of the global green house gas emissions are created by the United States. Majority of these emissions are generated from the coal-fired power plants, which is about 25 percent of total global emission [18,19]. In contrast, most of renewable energy resources produce little to no green house gas emissions.

Wind resources emit carbon-di-oxide between 0.02 and 0.04 pounds of CO<sub>2</sub>E/KWh, solar emits 0.07 to 0.2 pound of CO<sub>2</sub>/KWh, geothermal 0.1 to 0.2 pound of CO<sub>2</sub>E/KWh and hydroelectric between 0.1 to 0.5. Compare to renewable resources natural gas emits about 0.6 to 2 pound of CO<sub>2</sub>E/KWh and coal emits 1.4 to 3.6 pound of CO<sub>2</sub>E/KWh, which is much greater with respect to renewable resources. Renewable energy resources explore the feasibility to replace the carbon incentive energy resources and reduce the U.S. global warming emissions. For example, a 2009 UCS analysis found that a 25 percent of CO<sub>2</sub> emission is reduced by 2025 which is amount to 277 million metric tons annually by 2025 [20]. In addition, a ground-breaking study reveals that U.S. will produced 80 percent of its country's electricity from renewable sources by 2050 and found that green house gas emissions for the electricity production would be reduced approximately 81 percent [21].

**Improved public health and environmental quality:** Generating electricity from renewable resources have lower impact on public health as compared to conventional resources. The air and water pollutants that emit from coal fired plant and natural gas fired power plant create several health problem, such as breathing problem, neurological disorder, heart attack and cancer [22]. Wind, solar, hydroelectric plants produce no air pollutant while geothermal and biomass create small scale of air pollution but it is quite lower than that of coal and gas fired power plant.

There is no essential requirement of water for wind and solar energy production so it does not create water pollution. But coal and gas fired plants necessarily require water for steam production and other operation. Natural gas extraction by hydraulic fracturing require huge amount of water. Thus both coal and natural-gas fired power plants have significant impact on water resources. In addition hydroelectric plants affect the river's ecosystem both upstream and downstream to the dam. According to NREL (National Renewable Energy Laboratory) report water withdrawal for the purpose of geothermal

and biomass energy production will decrease about 51% to 58% by 2050 and water consumption also reduce by 47% to 55% [23].

### Stable energy prices:

Renewable energy is providing electricity at a affordable cost throughout the world and help in stabilizing the energy prices. The cost of solar panel has been reduced by 60% since 2011 and the generation cost of electricity from wind has dropped about 20 percent from 2010 to 2012 and more than 80 percent since 1980[24].

Only the installation cost is quite high for renewable plant but once built they operate at very low cost i.e. the running cost is low as for most technologies. As a result, renewable energy prices are relatively stable over time. Cumulative electricity and natural gas savings for consumers in all sectors will reach \$64.3 billion by 2025 and will grow to \$95.5 billion by 2030 [25].

In contrast, fossil fuel prices can vary drastically and are prone to substantial price swings. It is seen from Fig. 10 that the growth in saving electricity bill and natural gas bill is higher for commercial and residential sector compare to industrial sector [26]. The saving amount for residential sector is 48 billion \$, for commercial 40 billion \$ and for industrial it is about 10 billion \$.

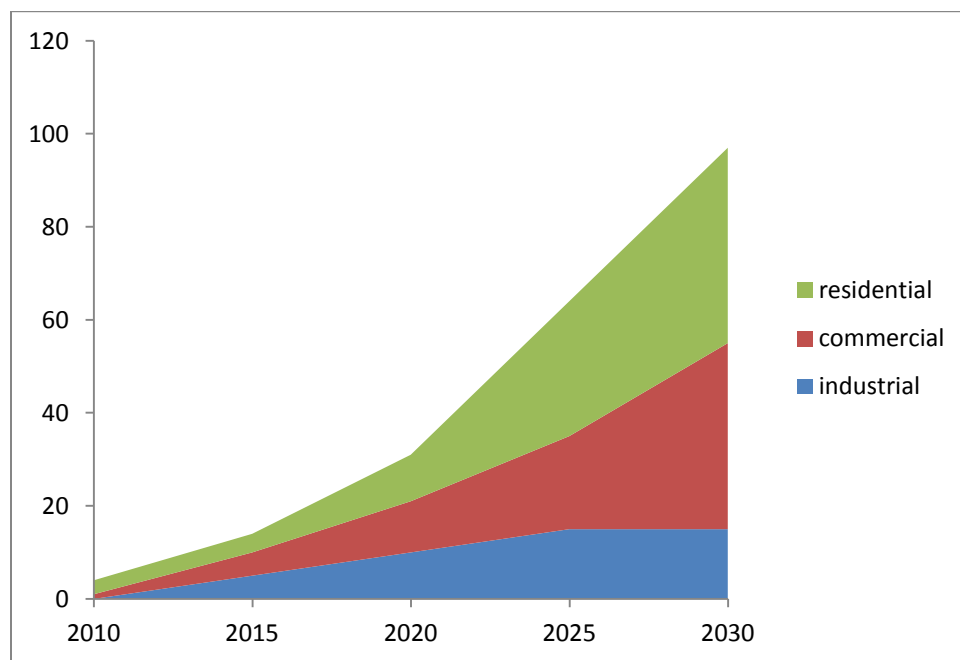


**Figure 10: cumulative electricity and natural gas bill saving by sector in (billion \$) [27]**

**A more reliable and resilient energy system:** Wind and solar system are less affected by the large scale weather disaster as they are distributed and modular. Since these renewable resources are distributed it is spread out all over the geographical area so, if weather disaster occur in any one location power will not cut off for all over the region and since it is modular that means it consist of several parts i.e. wind system consist of several individual wind turbine and the solar system consist of several solar array. If one of the parts is getting damage the remaining parts will continue the operation [28].

For example in 2012 Hurricane Sandy damaged coal fired power plant and suddenly stop the electric power generation and left million people without power for several hour in New York and New Jersey. Renewable energy resources are more reliable as compare to fossil fuel based resources. Coal, natural-gas and nuclear power plant consume large amount of water for cooling purpose and steam generation, but during draught due to limited supply of water the power station remain at risk in electricity generation. Since wind and solar photo voltaic system does not require water, so it remove the risk related to water scarcity and continue the electricity generation at any condition.

### **1.1.13 Status of clean energy development**

In our system mainly we use conventional energy. We receive this type of energy from coal, oil and natural gas, but due to increment of urbanization, demand of energy is increasing sharply. But due to the limited resources like Coal, Oil, we can't depend on those types of resources only. For Sustainable development of our society we have to use renewable energy.

These types of energy we get from clean resources which have much lower environmental impact. Renewable energy resource cannot be finished like other conventional sources. Due to increase in population energy demand uplifted gradually thus energy import increases which is very costly, but by using Renewable energy we can produce clean energy within the nation, so huge amount of money can be saved for local economic development and creating job prospect in a nation.

According to REN21's 2014 report renewable resources contribute 19 % to our global energy consumption and 22% to the electricity generation in 2012 and 2013 respectively. Worldwide investment in renewable technology is about US\$ 214 billion in 2013. Countries such as, china, United State are heavily investing in wind, hydro solar and bio fuel [34].

According to UNEP (United Nation Environmental Programme) in the past year (2015) the green energy investment is about \$270 billion. China is the highest investor in the renewable energy. It has been invested about \$83.3 billion, which is 39% more with respect to the year 2013. United State is the second

highest investor, invested about \$38.3 billion, which is 7 % more with respect to the year 2013 and Japan is the third highest investor, invested about \$35.5 billion, which is 10% more compare to the year 2013 [29].

The two biggest renewable energy investments is the solar and wind. The former accounting for \$149.4 billion, which is about 25 % more with respect to the year 2013 and the later is \$ 99.5 billion, about 11% of 2013 making a new record (fig:11).

Another big feature is the European offshore wind. Out of the seven projects the biggest investment is the 600 MW Gemini installations in water off the coast of Netherlands about \$ 3.8 billion.

In 2014 Brazil (\$7.6 billion), India (\$7.4 billion) and South Africa (\$5.5 billion) were all in the top 10 of investing countries in renewable resources. In view of this India has achieve about 4089.18 MW grid connected renewable energy generation in the FY-14-15 and about 93.16 MW<sub>EQ</sub> off grid. Muppandal wind farm in Tamil Nadu has the highest generation capacity is about 1500 MW. Charanka solar park in Gujarat has the highest generation capacity among the India's large photovoltaic power plant about 214 MW [30].

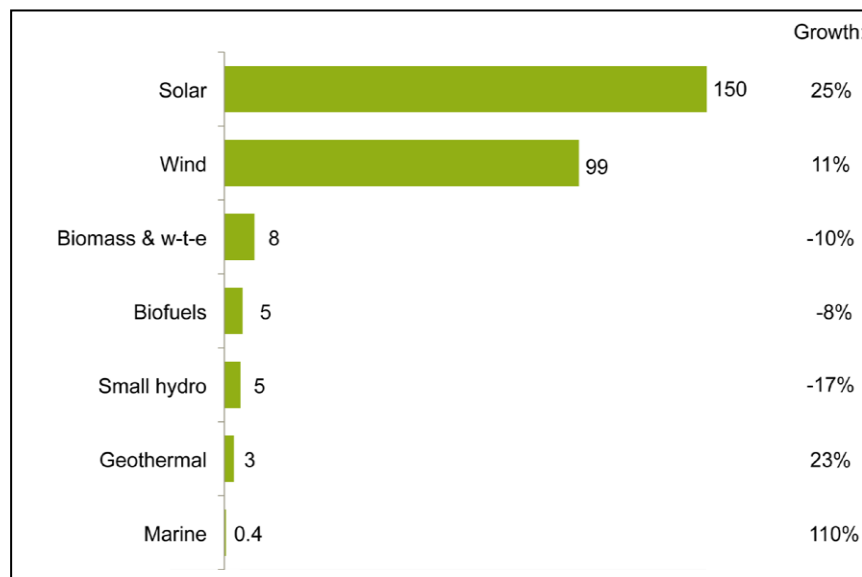


**Figure 11: Global new investment in renewable energy by source in 2014 and growth on 2013, in \$billion [31]**

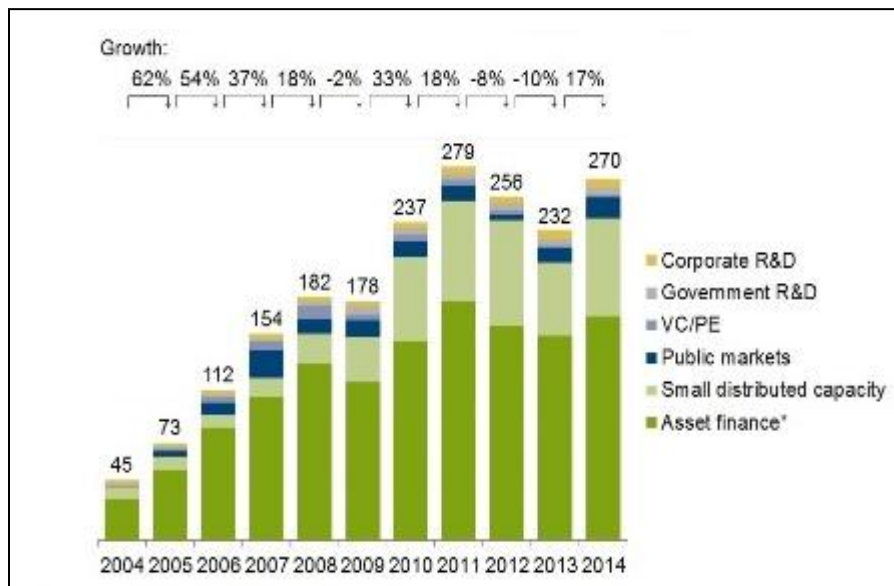


**Figure 12: Global investments in renewable energy by asset class, 2004-2014 [31]**

By the end of 2014, China, United States, Brazil, Canada, and Germany remained the top countries for total installed capacity in renewable power; the top countries for non-hydro capacity were again China, United States, and Germany, followed by Spain, Italy, and India [32]. (Fig.12) shows that global investment in renewable energy which is increased drastically from 2004 to 2014 and highest in the year 2011.

## 1.2 Importance of solar energy in the present context

The sun is one of the abundant resources of renewable energy. Solar energy can be huge enough to meet up the global energy crisis. The recent energy crisis and environmental burden are drawing enormous attention to solar energy utilization. Solar power has immense potential to bring in stability in the fluctuating electricity tariff, especially in India, as it is cheaper than the conventional thermal power in terms of operating cost.

In India about 3300-3700 hour of bright sunlight are available in a year in the north-west and west central region of the sub-continent and 2900 hour in central peninsular area, except in Assam, Kerala, and Kashmir where it is appreciably lower. About 7.5 kWh/m<sup>2</sup>/day of solar energy is received over the country as a whole. As it is ultra clean, natural and sustainable source of energy, it can be utilized for generating solar electricity, in solar heating and cooling appliances and in solar lighting [33].



**Advantages of solar power:**

- The major advantage of solar power is that no pollutant is created in the process of generating electricity. It does not pollute our air by releasing carbon-di-oxide, nitrogen-di-oxide, sulphur-di-oxide or mercury into the atmosphere like other traditional electricity generation process. Environmentally it is the most clean and green energy.
- It does not require any chemical fuel.
- Solar energy does not contribute to global warming, acid rain and smog formation. It actively contributes to decrease of harmful green house gas emission.
- There is no operating cost for the power it generates as solar radiation is free everywhere.
- Solar energy is economical in the long run, after the initial investment is recovered. Solar energy systems are virtually maintenance free and last for years.

The various applications for solar resources are as follows:

**Solar photovoltaic:** Photovoltaic, by far the most important solar technology for distributed generation of solar power, uses solar cells assembled into solar panels to convert sunlight into electricity. It is a fast-growing technology doubling its worldwide installed capacity in every couple of years. PV systems range from distributed, residential, and commercial rooftop or building integrated installations, to large, centralized utility-scale photovoltaic power stations. Commercially we use three type of photo voltaic modules: mono-crystalline module, polycrystalline module which is less efficient and less expensive to produce electricity and thin film module normally used for running consumer devices [34]. Thin film PV technologies offer the advantage of providing lightweight and unbreakable panels on flexible substrates that can be integrated with the roof. Solar PV technologies can operate up to 30 years, and are used worldwide. The global PV market is currently growing at a rate of approximately 20 to 25 percent per year [25].

PV solar systems range in size from 50 watts to one kW for stand-alone systems (usually with battery storage) and 500W to five kW for grid-connected systems or larger remote water pump systems. PV modules can also be integrated with diesel, wind and hydro systems and are cost-effective in comparison with other energy sources in remote areas without having access to electrical grids. PV panels are used for charging batteries in lanterns, village lighting, communications, refrigeration and water pumping. PV modules typically cost between \$2.50 to \$3.00/watt [35]..

**Solar thermal heating:** The application area for solar thermal energy extends from simply heating water to so called combi-system which can also be used for room heating. This application mainly

applied for residential building. The availability of solar heat depends clearly on sun. The use of solar heat relies on heat storage because solar energy availability fluctuates from day to night and seasonally as result of weather. It is important that available solar energy should be collected and stored in the storage tank and used whenever heat needed. The different applications of solar heating are water heating and space heating.

Solar collector area used for combi-system is larger. This also helps to heat building in spring and autumn. The collector area required in this case is also depending on weather condition and the consumer demand. The solar fraction of total heating requirement for the building is typically 20-30 percent, depending on how well the building is insulated and how high the requirement is [36].

**Solar thermal cooling:** The term solar cooling refers to the devices and processes that use solar energy for cooling. Solar cooling system has the advantage of using predominantly non-toxic and environmentally sound working fluid such as water or salt solution and can be used for stand alone system.

The available solar energy, in the form of solar radiation flux is utilized by the solar panel, in order to produce high temperature fluid that is accumulated in solar tank. The chiller the real heart of the process, use the hot fluid of the storage tank to produce a cold fluid, the cold fluid can then be used in the normal cooling plant, similar to electrical refrigeration. The capacity of solar cooling devices at its peak when the solar insolation i.e. the solar irradiance is highest.

This work mainly based on solar cooling application i.e. solar absorption refrigeration system. To begin with solar driven absorption refrigeration system we should have knowledge about refrigeration cycle and system.

### 1.3 Refrigeration cycle

There are two types of refrigeration cycle:-

- Vapor-compression refrigeration cycle
- Vapor-absorption refrigeration cycle

#### 1.3.1 Vapor-compression refrigeration cycle:-

The vapor compression refrigeration cycle is the most widely used cycle for refrigeration, air-conditioning system and heat pump. It consists of four processes:-

1-2 isentropic compression in a compressor

2-3 Constant pressure heat rejection in a condenser

3-4 Throttling in the expansion device

4-1 Constant pressure heat absorption in an evaporator

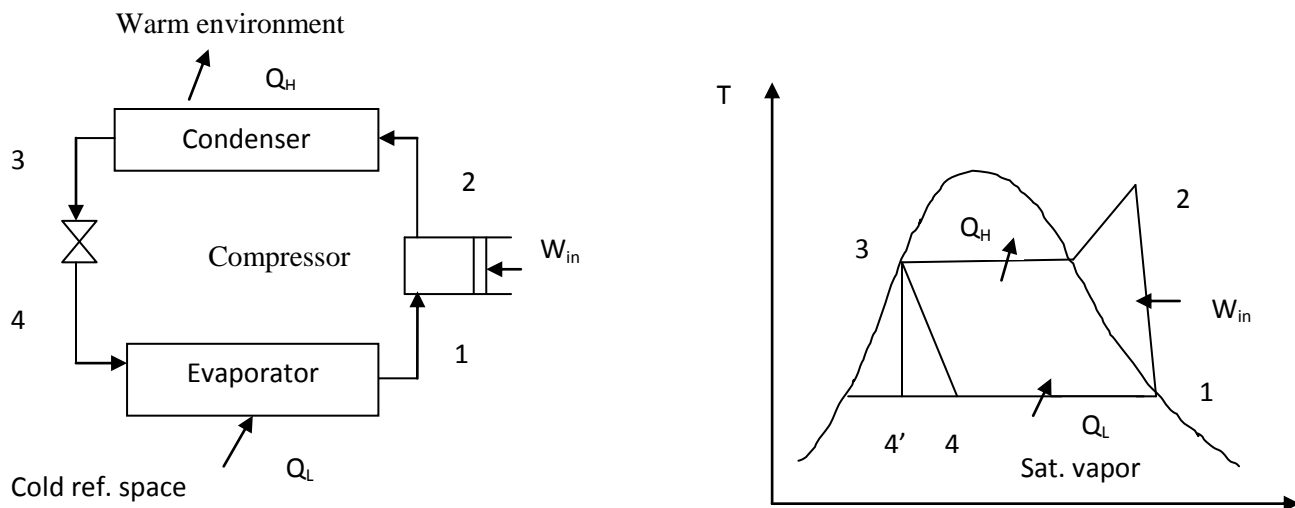


**Figure 13: Vapor compression refrigeration cycle**

s

In the above vapor – compression refrigeration cycle (Fig. 15) the refrigerant enters the compressor at state 1 as saturated vapor and is compressed isentropically to the condenser pressure. The temperature of refrigerant increases during this isentropic compression process to well above the temperature of surrounding medium. The refrigerant then enters the condenser as superheated vapor at state 2 and leave as a saturated liquid at state 3 as a result heat rejection to the surrounding. The temperature of refrigerant at this state is still above the temperature of the surrounding.

The saturated liquid refrigerant at state 3 is throttled to the evaporator pressure by passing it through the expansion valve or capillary tube. The temperature of the refrigerant drops below the temperature of the refrigerated space during this process. The refrigerant enters the evaporator at state 4 as a low quality saturated mixture, and it completely evaporates by absorbing heat from the refrigerated space. The refrigerant leaves the evaporator as a saturated vapor and reenters the compressor, completing the cycle. The coefficient of performance (COP) is defined as follows

$$COP = \frac{Q_L}{W_{net}} = (h_1 - h_4)/(h_2 - h_1) \quad (1)$$

### 1.3.2 Vapor-absorption refrigeration cycle:-

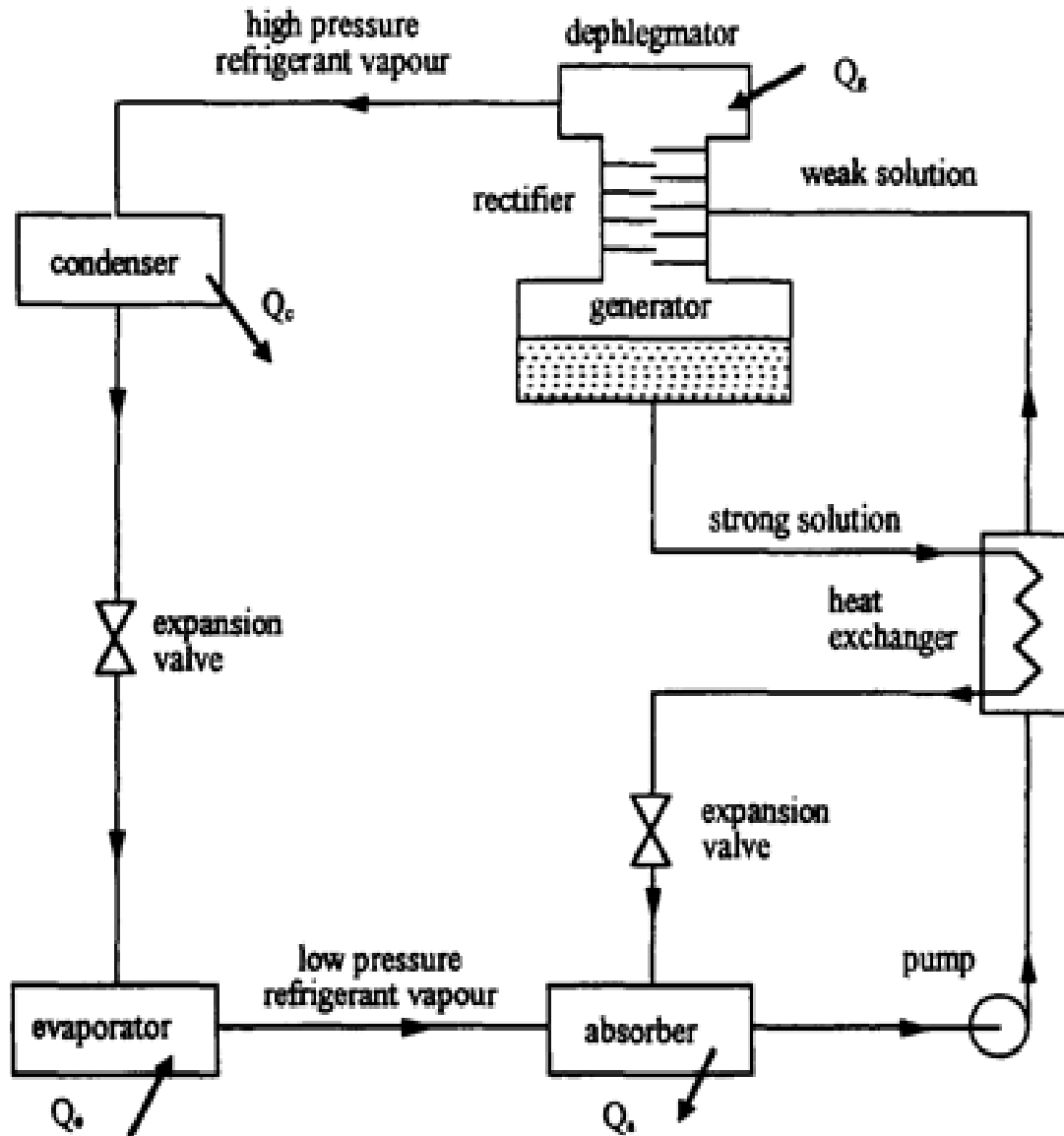


Figure 14: Absorption refrigeration cycle [37]

Another form of refrigeration that becomes economically attractive when there is a source of inexpensive thermal energy source at a temperature of 100 to 200°C is vapor absorption refrigeration. Some examples of inexpensive thermal energy sources include geothermal energy, solar energy, waste heat from cogeneration processes etc.

As the name implies absorption refrigeration system involves the absorption of a refrigerant by a transport medium or absorber. The most widely used absorption refrigeration system is the ammonia – water system, where ammonia serves as refrigerant and water as the transport medium. Other absorption refrigeration system includes water-lithium bromide and water –lithium chloride system where water serve as the refrigerant. The latter two systems are limited to application such as air conditioning where the minimum temperature is above the freezing point of water.

It is evident from the above cycle (Fig. 16) that this system looks very much like vapor compression system, except that the compressor has been replaced by a complex absorption mechanism consisting of an absorber, a pump, a generator and a regenerator or heat exchanger. Low pressure ammonia vapor leaving the evaporator is absorbed by the liquid strong solution in the absorber. This is an exothermic reaction, thus heat is released during this process. The amount of  $\text{NH}_3$  that can dissolve in  $\text{H}_2\text{O}$  is inversely proportional to the temperature. Therefore it is necessary to cool the absorber to maintain its temperature as low as possible. The pump receives the low pressure liquid weak solution from the absorber, elevate the pressure of the weak solution and deliver it to the generator. In generator, heat from the high temperature source drives of the refrigerant vapor from the weak solution. The liquid strong solution returns to the absorber through the regenerator where it transfers some heat to the liquid weak solution and leaving the pump and throttling to the absorber pressure. The high pressure refrigerant vapor condenses into liquid in the condenser and enters the evaporator through throttling valve, maintaining the pressure difference between the condenser and evaporator. In order to improve cycle performance, a solution heat exchanger is normally added to the cycle as shown in fig:16, it is an energy saving component not essential for successful cycle operation.

The heat flow pattern to and from the four heat exchange components in the absorption cycle is that high-temperature heat enter the generator, low temperature heat from the substance being refrigerated enter the evaporator. The heat rejection from the cycle occurs at the absorber and condenser at a atmosphere temperature. However, for the  $\text{H}_2\text{O}/\text{NH}_3$  absorption cycle, it not only consists of all the four components previously describe, but also rectifier and dephlegmator as shown in fig: 16. The need for these two components is by the fact that water is volatile. When this water enter the evaporator, it elevate the evaporating temperature, it may freeze in the pipeline also. To remove much water vapor as possible, the vapor driven off at the generator is first flow countercurrent to the incoming solution in the rectifier, and then the solution passed through the dephlegmator and condenses some water –rich liquid draining back to the rectifier. Through this process only small amount of water vapor escape the dephlegmator and passes through the evaporator to the absorber [37].

The cycle performance is measured by coefficient of performance (COP), which is defined as the refrigeration rate over the rate of heat addition at the generator plus the work input to the pump, that is

$$COP = Q_e / (Q_g + W_p) \quad (2)$$

### 1.3.3 Advantages of vapor-absorption refrigeration cycle

- ❖ In absorption refrigeration system a liquid is compressed instead of vapor. The steady flow work is proportional to its specific volume. Since the specific volume of liquid is less than vapor the work input of absorption refrigeration system is very small.
- ❖ The vapor absorption system runs mainly on the waste or extra heat in the plant. Thus one can utilize the extra steam from boiler, solar heat or waste heat from cogeneration process. In case of vapor compression refrigeration process the compressor can run only by electric power supply, no other type of energy can be utilized in this system.
- ❖ The vapor compression refrigeration system can run only on electric power and they require large amount of power. These days the electric power is very expensive, hence the running cost of vapor compression refrigeration system is very high. In case of absorption refrigeration system small pump is used and thus the require electric power is quite low. In most of the process industries where absorption refrigeration system is used, there is some extra steam available from the boiler, which can be used for running the system.
- ❖ The compressor of the vapor compression system is operated at very high speed and it makes lots of vibration and noise. It also requires very strong foundation so that it can remain intact under vibration and high pressure of the refrigerant. In the absorption refrigeration system there is no major moving parts hence they don't vibrate, don't make noise and also don't require heavy foundation. The absorption refrigeration system operates silently.
- ❖ In ammonia water absorption refrigeration system, ammonia is used as the refrigerant, which is easily and cheaply available. In lithium bromide system water is refrigerant which is also cheaply available. In case of vapor compression refrigeration system halocarbon are used as refrigerant which is very expensive.
- ❖ Most of the halocarbon refrigerant used in the vapor compressor refrigeration system produces green house effect. As per the Montreal Protocol, there use has to be stop completely by the year 2020. In the absorption refrigeration system no refrigerant produce the green house effect, so there use would not be stop in future.

### 1.3.4 Limitation of vapor absorption refrigeration cycle

- ❖ Though the running cost of the absorption refrigeration system is much lesser than the vapor compression system, its initial capital cost is much higher.
- ❖ In the lithium bromide absorption refrigeration system, lithium bromide is corrosive in nature, which reduces the overall life of the system. In case of the ammonia system, ammonia is corrosive to copper. In the vapor compression system copper is used with the halocarbon refrigerants and they are quite safe thus ensuring long life of the refrigeration system. As such the vapor compression system with reciprocating or centrifugal compressor has longer life than the lithium bromide absorption refrigeration system.
- ❖ The working pressure of the absorption refrigeration cycle is very low. In case of the lithium bromide system these pressures are so low that even the expansion valve is not required since the drop in pressure of the refrigerant due to its flow is good enough to produce its expansion. Due to this the refrigeration system should be sealed thoroughly so that no atmospheric gases would enter the refrigeration system. As such the system of the compression refrigeration should also be packed tightly, but this is to prevent the leakage of the refrigerant to the atmosphere.
- ❖ The coefficient of performance of the absorption refrigeration systems is very low compared to the vapor compression systems. For instance, the COP of the two stage lithium bromide system is about 1.1, while that of the vapor compression system used for the air conditioning applications it is about 4 to 5. Thus the absorption refrigeration system becomes competitive only if the ratio of the electricity to fuel (oil, gas or coal used to generate the steam in the boiler) becomes more than four. If this ratio is lesser there are chances that excess fuel would be required to generate the steam. However, if there is excess steam in the industry, this ratio may not be given importance.
- ❖ In the absorption refrigeration heat has to be rejected from number of parts like condenser, absorber, analyzer, rectifier etc. thus heat rejection factor for absorption refrigeration system is high and it can be around 2.5. In the compression refrigeration system the heat is given up only from the condenser, so its heat rejection factor is small, which is about 1.2. Thus the cooling tower and pump capacities for pumping the cooling water have to be higher in case of the absorption refrigeration system, which leads to increase in the running cost of the system.

### 1.3.5 Different working fluid used in absorption refrigeration cycle

**Table 5: Different working fluid used in absorption refrigeration system is as follows:**

Working fluid	refrigerant	absorbent
NH <sub>3</sub> -H <sub>2</sub> O	NH <sub>3</sub>	H <sub>2</sub> O
NH <sub>3</sub> -LiNO <sub>3</sub>	NH <sub>3</sub>	LiNO <sub>3</sub>
NH <sub>3</sub> -NaSCN	NH <sub>3</sub>	NaSCN
LiBr-H <sub>2</sub> O	H <sub>2</sub> O	LiBr

The advantage of using NH<sub>3</sub>-H<sub>2</sub>O as a working fluid is that :

- ❖ Since ammonia used as refrigerant this system can be used both as refrigerator and air-conditioning system application. Where as water/lithium bromide does not use for refrigeration there is a problem of crystallization. Since freezing point of ammonia is -77°C so the evaporator temperature can go below 0°C i.e. -10°C to -12°C. Where as for water/lithium bromide solution where water is the refrigerant we cannot make the evaporator temp below 0°C [38].
- ❖ They are available in very small large refrigeration capacities in application ranging from domestic refrigeration to large cold storage.
- ❖ Ammonia is not compatible with copper and its alloy because it get cored in presence of ammonia. The entire system fabricated out of steel.
- ❖ Another important difference between this system and water/lithium bromide system is that the operating pressure. Lithium bromide/water system operating at very low pressure (high vacume), the ammonia water system operating at a pressure much higher than atmospheric thus the problem of air leakage is eliminated.
- ❖ Also NH<sub>3</sub>/H<sub>2</sub>O system does not suffer from crystallization problem that is encountered in a water-lithium bromide system
- ❖ However ammonia is toxic and inflammable so system needs safety precaution.



### 1.3.6 Collection of solar energy and classification of solar collector

Energy is considered a prime agent in the generation of wealth and a significant factor in economic development. The importance of energy in economic development is recognized universally and historical data verify that there is a strong relationship between the availability of energy and economic activity. Although at the early 70s, after the oil crisis, the concern was on the cost of energy, during the past two decades, the risk and reality of environmental degradation have become more apparent. The growing evidence of environmental problems is due to a combination of several factors since the environmental impact of human activities has grown dramatically. This is due to the increase of the world population, energy consumption and industrial activities. Achieving solutions to environmental problems that humanity faces today requires long-term potential actions for sustainable development. In this respect, renewable energy resources appear to be one of the most efficient and effective solutions [39].

The most available source of renewable energy on earth is solar energy as the earth receives million of watts of energy everyday coming from solar radiation. However, only a fraction of it in the form of day lighting and photosynthesis is used by the natural world, one third is reflected back into space and rest is absorb by land, ocean, and cloud. Thus it is very reasonable to collect solar energy and utilize it to generate electrical power, heat and cooling appliances. The effect of using solar energy on the environment for variety of application is minimal as it produces no harmful effect. Solar energy is the appropriate energy source to meet the increasing demand of energy worldwide. Researcher have investigated and develop technologies on how to harvest solar energy to serve human beings and are still considering new technologies to maximize the collection and utilization of solar energy.

There are particular challenges in the effective collection and storage of solar energy though it is free of taking. As solar radiation is only available during daytime, the energy must be collected in efficient manner and then must be stored. Solar thermal collectors are the existing component to capture solar radiation which is then turned to thermal energy and transferred to working fluid subsequently. Therefore solar collector is the main and most critical component of any solar system [40]. There are basically two types of solar collector. Stationary and tracking. The classification of solar collector is given below,

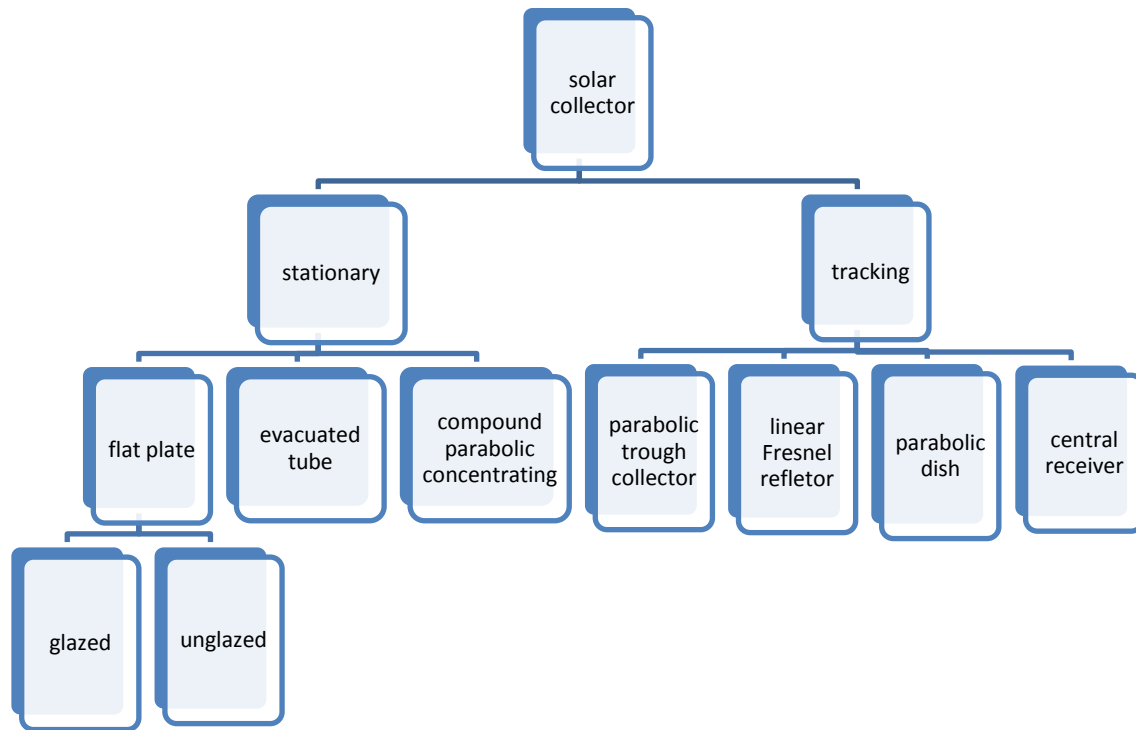


**Figure 15: Classification of solar collector**

### 1.3.7 Advantages of using evacuated tube solar collector

According to many researchers evacuated tube solar collector (ETSC) has much more efficiency than flat plate collector (FPC). Evacuated tube solar collector can collect both direct and diffuse radiations. Besides excellent thermal performance, ETSCs have convenient installation and easy transportability.

The peak energy output is provided by an FPC only at mid-day when the sun is perpendicular to the surface of the collector whereas the evacuated tube solar tubes are able to track sun passively throughout the day because of the cylindrical shape of the evacuated tube. The incident angle of sunlight on the cylindrical tubes is at  $90^\circ$  throughout the day. Hence the peak absorption is captured by ETSCs all over the day. Thus the heat loss in evacuated tube is much less than FPC where convective and conductive heat loss occurred. It is noted that the ETSCs is less affected by the low temperature and wind because of the vacuum envelop between the inner and outer tubes of evacuated pipe. The vacuum is formed to reduce the convective and conductive heat loss by evacuating the air inside the interior tube of the ETSC. The maintenance of ETSCs is easy and inexpensive. If the tube is damaged or broken, the system does not stop working, the collector still operate at a lower efficiency i.e without shutting down the whole system it is possible to replace the damaged tube whereas for the FPC if the collector is

damaged, the entire system needed to be shut down to replace the collector. An evacuated tube solar collector is able to generate heat quickly and the emissivity is lower for an evacuated collector whereas for an FPCs emissivity is higher [40].

### 1.3.8 Evacuated tube solar collector

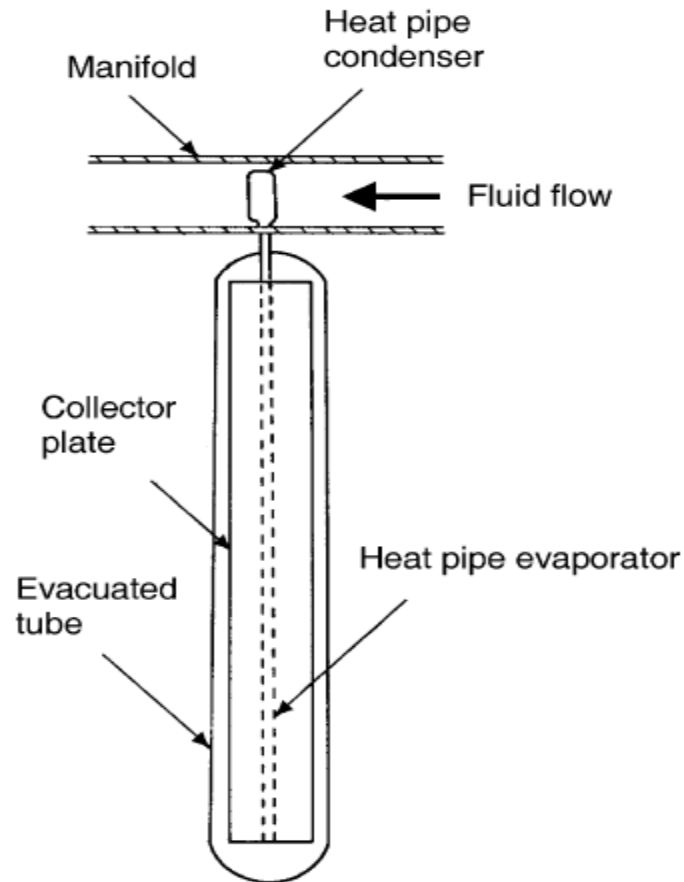


**Figure 16: Schematic diagram of evacuated tube collector [40]**

Conventional simple flat plate solar collector is developed for use in sunny and warm climate. Their performance however greatly reduce when condition become unfavorable during cold, cloudy and windy days. Evacuated heat pipe solar collectors operate differently than other collector available in the market. These solar collectors consist of heat pipe inside a vacuum- sealed tube, as shown in Fig.17.

Evacuated tube collector basically consists of heat pipe inside a vacuum sealed tube. The vacuum envelope reduces convection and conduction losses, so the collectors can operate at higher temperatures than FPC. Like FPC, they collect both direct and diffuse radiation. However, their efficiency is higher at low incidence angles. This effect tends to give ETC an advantage over FPC in day-long performance.

ETC use liquid–vapor phase change materials to transfer heat at high efficiency. These collectors feature a heat pipe (a highly efficient thermal conductor) placed inside a vacuum-sealed tube. The pipe, which is a sealed copper pipe, is then attached to a black copper fin that fills the tube (absorber plate). Protruding from the top of each tube is a metal tip attached to the sealed pipe (condenser). The heat pipe contains a small amount of fluid (e.g. methanol) that undergoes an evaporating-condensing cycle. In this cycle, solar heat evaporates the liquid, and the vapor travels to the heat sink region where it condenses and releases its latent heat. The condensed fluid return back to the solar collector and the process is repeated. When these tubes are mounted, the metal tips up, into a heat exchanger (manifold) as shown in Fig. 18 [39].

## 1.4 Literature Review

### 1.4.1 State of art for absorption refrigeration system

Energy is considered as the major agent in the generation of wealth and an important factor in economic development. With developing technology the rapid increase in world population, increasing thermal load, life standard and comfort demand in conjunction with architectural characteristic and trend, the demand for energy and its use for cooling are ever increasing. In summer particularly under tropical climate, air conditioning has highest energy expenditure in building. During recent year, research aimed at development of technologies that can offer reduction in energy consumption, peak electrical demand and energy cost without lowering the desire level of comfort. Considering such condition alternative cooling technologies such as heat driven absorption refrigeration system is develop. Also as in the recent year depletion of ozone layer and green house effect become serious problem and conventional working fluid of vapor compression system are causing ozone layer depletion and green house effect. Therefore many researches devoted towards absorption refrigeration system as they are environmentally friendly and cause no depletion of ozone layer and global warming and can be driven by low grade source of energy such as solar or waste heat [41].

Many studies have been dealt on thermodynamic analysis and performance evaluation of absorption refrigeration system. Among these studies **Mazzie et al. [42]** present an optimization of a single effect absorption refrigeration system by developing nonlinear mathematical modeling. The result from the mathematical modeling consist show that COP increases with total heat transfer area, flow rate of refrigerant is decreasing and flow rate of strong and weak solution is increasing with total heat transfer area for a given cooling capacity of 50 KW. A 70 KW cooling capacity water / lithium bromide solution absorption cooling system is modeled by **Ketfi et al.[43]** the result show that the performance coefficient is increase with generator and evaporator temperature and effectiveness of heat exchanger and decreases with condenser and absorber temperature. The heat exchanger effectiveness reaches at maximum value of

0.8 to 0.85. The same result has been evaluated by **Lamine et al.[44]** for the same system operating in industrial manufacturing of detergent, but in this study COP is constant beyond 15°C of evaporator temperature and begin to decline above 90°C of generator temperature. Theoretical and experimental investigation on absorption refrigeration system for acetone-ZnBr<sub>2</sub> solution is presented by **Karno and Ajib[45]**. From the evaluated result it is confirmed that the system operating in generator temperature of 50°C without any inconvenience. Thus it can be considered as the suitable solution for moderate source of temperature. It is found that the COP achieve as 0.4 (by measuring) and 0.6 (by simulation). Ferreira carried out a study on thermodynamic and physical properties of ammonia-lithium nitrate (NH<sub>3</sub>-LiNO<sub>3</sub>) and ammonia-sodium thiocyanate (NH<sub>3</sub>-NaSCN) solution and interesting comparison among NH<sub>3</sub>-H<sub>2</sub>O, NH<sub>3</sub>-LiNO<sub>3</sub> and NH<sub>3</sub>-NaSCN solution in done by **sun[46]** and **Abdulateef et al.[47]**. Among ammonia based solution although NH<sub>3</sub>-NaSCN can be considered as alternative solution to NH<sub>3</sub>-H<sub>2</sub>O, Sun [46] emphasized that this solution can not be used for evaporator temperature below -10°C due to the problem of crystallization. Then **sun [37]** carried out a study on both ammonia-water (NH<sub>3</sub>-H<sub>2</sub>O) and water-lithium bromide (H<sub>2</sub>O-LiBr) absorption refrigeration system. He has presented the thermodynamic properties of the two cycles. The result shows in this studies is contradict with his previous work. In this study both for water-lithium bromide and ammonia-water solution COP decreases with generator temperature but in his previous work the same has been increases with generator temperature for NH<sub>3</sub>-H<sub>2</sub>O solution. A detailed thermodynamic study on H<sub>2</sub>O-LiBr absorption refrigeration cycle is done by **Kaynakil and Kilic [48]**. The influence of operating temperature and effectiveness of heat exchanger (SHE and RHE) on thermal load on different component, coefficient of performance (COP) and efficiency ratio were investigated. The same type of study done by **Karamangil et al. [49]**, but the extra things he has done is consider different working fluid pair with H<sub>2</sub>O-LiBr i.e. NH<sub>3</sub>-H<sub>2</sub>O and NH<sub>3</sub>-LiNO<sub>3</sub>. He also added another heat exchanger to the system, solution refrigerator heat exchanger (SRHE). He examined that the performance of the system was affected from SHE more than RHE and SRHE. While the use of SHE improve the system COP up to 66%, RHE and SRHE have an effect of only 14% and 6%. **Cai et al. [50]** presented a dynamic model of ammonia/water absorption refrigeration system. The result shows that the coefficient of performance of the system and the mass flow rate ratio of the system decreases with generator temperature. The same variation done with respect to absorber temperature, the 1<sup>st</sup> one is decreases and the 2<sup>nd</sup> one is increases. **Jain et al. [51]** carried out a study for cascaded vapor compression-absorption system (CVCAS). It consist of a vapor compression refrigerator system (VCRs) coupled with vapor absorption refrigeration system. The result show that the electric power consumption in CVCAS is reduced by 61 % and COP of the compression section improve by 155% with respect to the corresponding values pertaining to a conventional VCRs.

### 1.4.2 State of art for solar driven absorption cooling system

The possible use of solar energy as the main heat input for a cooling system has led to the several studies of available cooling technologies that use solar energy. Various types of solar powered system are available for cooling applications. One wide spread application of a solar-powered system is for absorption cooling which is an alternative approach to cooling that is largely thermally driven and require little external work. Recently solar energy has received interest as an alternative energy source for cooling system, especially in place where electricity is expensive or in short supply. With the usage of solar energy, usages of conventional energy sources and its peak demand will be reduced.

**Ozgoren et. al. [41]** carried out a study on hourly performance investigation on solar absorption refrigeration (SAR) system with evacuated tube collector and ammonia-water (NH<sub>3</sub>-H<sub>2</sub>O) solution. Here the hourly variation for solar radiation data and atmospheric or ambient temperature is given. Firstly the variation of various parameters such as ideal and actual performance efficiency, condenser capacity and heat transfer rate in the generator and absorber during the day is calculated for different cooling capacities and generator temperature. According to the obtained result the SAR system is considerably suitable for home/office cooling purpose between the hour 9.00 and 16.00 without considering storage tank. The most suitable performance of the SAR system is calculated for the generator temp equal to or higher than 110°C and the COP<sub>cooling</sub> is inversely proportional to the atmospheric air temperature. Evacuated tube collector area for a 3.5 KW cooling load capacity is found to be 35.95 m<sup>2</sup> for the region at 16.00 whereas it is 19.85 m<sup>2</sup> at 12.00. **Salesh et. al. [52]** and **Atmaca et.al. [53]** Considered storage tank for modeling a solar absorption refrigeration system but they used different collector, the first one design the system for flat plate collector and the second one design the system for evacuated tube collector, but evacuated tube collector is more efficient than that of flat plate collector. Both of them use water-lithium bromide as the working fluid of the SAR system. **Siddiqui et. al. [54]** carried out a study on alternate design for a 24-h operating solar-powered absorption refrigeration technology. The analysis indicates that out of four alternate designs continuously operating solar-powered aqua-ammonia absorption system with refrigerant storage is the most suitable alternative design for an uninterrupted supply of cooling effect. In this study the influence of generator temperature and evaporator temperature on performance coefficient of all alternate design and optimum design is shown. **Zurigat et.al [55]** describes the performance of a 1.5 ton solar-operated absorption refrigeration unit operating with a 14 m<sup>2</sup> flat-plate solar collector area and containing five heat exchanger: the generator, the absorber, the condenser, the solution heat exchanger and finally the evaporator. This is an experimental unit where the condenser and absorber both cooled by city main water. This is the particular unit, called second generation unit that compared with the first generation low cost, locally manufactured, 0.5 ton capacity unit. The influence of generator and

evaporator temperature on actual and theoretical coefficient of performance is evaluated. The result shows that the maximum values obtained for both actual and theoretical coefficient of performance were 0.85 and 2.7 respectively. **Ghaddar et. al [56]** performed an analytical study on solar energy application of solar space cooling in residential area using solar driven lithium bromide absorption refrigeration system. The results evaluated from the have shown that for each ton of refrigeration it is required to have a minimum collector area of 23.3 m<sup>2</sup> with an optimal water storage tank capacity ranging from 1000 to 1500 liters. The system operates solely 7 hour in a day based on solar energy. The monthly solar fraction of total energy used for cooling is determined as a function of solar collector area and storage tank capacity. **Assilzadeh et.al [57]** and **Iranmanesh et.al [58]** both represent a model solar driven water-lithium bromide absorption refrigeration system but first one use TRANSYS software and the second one use genetic algorithm. In the first paper the result show that the system is in phase with weather i.e. the cooling demand is high when the solar radiation is high. For continuous operation and increase the reliability of the system 0.8 m<sup>3</sup> storage tank is necessary. For refrigeration load of 1 ton or 3.5 KW system 35 m<sup>2</sup> evacuated tube collector with slope 20°. **Iranmanesh et.al [58]** also used evacuated tube collector with optimum angle to get as much as solar irradiance. Two objective functions are considered for genetic algorithm namely auxiliary energy and net profit obtained from the solar system. The computer code develops to minimize the auxiliary energy and maximize the net profit. **Weber et. al [59]** proposed a solar driven ammonia water absorption chiller model for concentrating solar collector. Fresnel collector provides the driving temperature to the generator of the chiller up to 200°C. The chilled water temperature is produce in the range -12°C and 0°C.

#### **1.4.3 State of art for solar driven air conditioning system**

According to internal energy agency (IEA) the world energy demand will increase by 35 percent from 2010 to 2035. This increase is associated with world population growth and economic growth especially in developing countries. Increasing energy demand lead to more green house gas emission and accelerated global warming. In the year 2012, the average temp across the U.s was 3.2°C higher than that of normal. Hotter weather and economic growth will result in more use of air conditioning system and contribute to accelerated energy demand. Now the building cooling by conventional electricity-powered air-conditioning system leads to increase green house gas emission and more fossil fuel harnessing. One of the solution for addressing world wide energy demand increase and climate change will be utilising renewable energy to provide cooling for air-conditioning system. In this scenario researcher has been focused on solar cooling or solar air-conditioning system [60]. Solar driven cooling system can cope with solar collector working in a wide range of temperature. **Wang et. al [61]** presented five cooling system including modular silica-gel water adsorption chiller which have 50 KW capacity and COP over 0.4. The

system consist of two adsorber which can alternate between adsorption and desorption phases to realize continuous cooling via switching the hot/cooling water valve. 2<sup>nd</sup> one is the single/double effect LiBr-water absorption chiller which does not work continuously due to instability of solar power, usually an auxiliary heat source like gas firing boiler or electrical boiler is added, but this is inefficient as the system has low COP. The system consists of low pressure generator, high pressure generator, condenser, absorber, evaporator and sol. Heat exchanger. It can work in the both mode i.e. single effect and double effect mode. It has heat source temperature 80-95°C. 3<sup>rd</sup> one is the 1.n.effect LiBr-water absorption chiller which is drive in a single effect mode with a heat source temperature 90-135°C. 4<sup>th</sup> one is the CaCl<sub>2</sub>/AC (Activated Carbon) – ammonia absorption refrigeration with heat source temperature 100-140°C. Last but not the least is the water-ammonia absorption ice maker with a heat source temperature is 140-170°C which have better internal heat recovery system. The result shows that how the collector efficiency and total solar fraction vary with storage tank specific volume. Still now we have studied that **Ghaddar et. al [56]**, **Assilzadeh et. al [57]** and **Iranmanesh et. al [58]** develop model for solar driven LiBr-water absorption cooling system, out of them **Ghaddar et. al [56]** modeled the system for space heating. We have mainly seen that researcher mainly model LiBr-water absorption cooling system and ammonia-water absorption cooling system either they use as refrigeration or space cooling or water chiller. **Shirazi et. al [62]** investigated in the present work different design and operational modes for solar heating and cooling absorption chiller system. Three control scenarios are proposed for solar collector loop. The first uses a constant flow pump, while the second and the third control scheme employ a variable speed pump, where the solar collector set point temp could be either fixed or adjusted to the required demand. A TRNSYS software model is used for investigating the system. Simulation result revealed that the total solar fraction of the plant increase by up to 11% when variable speed solar pump used for adjusting the set point temperature instead of constant flow pump. Another finding from the study is that auxiliary heater in parallel with storage tank enhance the plant solar fraction and collector efficiency up to 13% and 9%. **Vinas et. al [63]** represented a model on LiBr-water absorption cooling system for costal zone in Mexico. They use TRNSYS software for developing the model. Evacuated tube collector with are 207 to 220 m<sup>2</sup> is use for collecting the solar heat. The result presented hourly variation of useful & auxiliary heat and the variation of solar fraction with respect to different collector area. So far more commonly system used are single-effect water/lithium bromide absorption chiller powered by flat plate or evacuated tube collector operating with COP of about 0.5-0.8 and driving temperature of 75-95°C. **Cabrear et. al [64]** carried out a study on water/lithium bromide solar air conditioning system driven by parabolic trough collector (PTC). PTC are parabolic concentrating system that focus the direct solar radiation parallel to the collector axis onto a focal line. A receiver pipe installed in this focal line with a heat transfer fluid flowing inside it that absorb concentrated solar energy from the pipe wall and raises its enthalpy. The



collector provide with one axis solar tracking system to ensure solar beam fall on parallel to this axis. The result presents the influence of different storage capacity on soar fraction of an office building in Madrid. **Kanan et. al [65]** represent a model salinity gradient solar pond is suggested as a collector to drive absorption chiller , where chilled water passing through a cooling coil and the cool air distributed by a fan to 125 m<sup>2</sup> single family house in Baghdad, Iraq. MATLAB and TRNSYS software is used for simulating the system. Here the chilled water outlet temperature for different solar pond area for two year simulation time is presented. With the 250 m<sup>2</sup> pond area the chilled water outlet temperature does not stabilize at the set point even in the second year, but with 400 m<sup>2</sup> pond area, the chilled water outlet temp stabilize at the set point at the end of 1<sup>st</sup> summer. Thus 400 m<sup>2</sup> suggested as the suitable pond are for this 125 m<sup>2</sup> single family house. From the figure of water inlet temperature to the absorption chiller, it is find that when the hot water inlet temperature is 70°C or higher, then absorption chiller work normally and chilled water temperature close to set point temperature. **El-Shaarawi et. al [66]** analysed alternative design for 24-hour operating solar-powered lithium bromide (LiBr)- water absorption airconditioning system. Three alternative design heat storage, cold storage and refrigerant storage are studied. The result indicate that continuously operating solar-powered LiBr-H<sub>2</sub>O absorption with refrigerant storsge is the most suitable design for 24-hour cooling effect.

### 1.5 Scope of present work

The present work is based on solar driven ammonia-water absorption cooling system for the purpose of air-conditioning of a office space with necessary storage capacity. The solar energy is captured using evacuated tube collectors, which has high efficiency and no convective loss due to the vacuum existing in the annular space between two concentric glass tubes.

Firstly, a detailed analysis of ammonia-water vapor absorption system has been done, by varying the temperature of generator, absorber, condenser and evaporator, to determine the optimum operating parameters that give the maximum COP of the system. The parameters for the highest COP have been selected to run 10 numbers of 2 ton air-conditioners for 10 hour operation in a day under summer conditions for an office space in Kolkata. The collector area has been calculated along with the variation of the temperature of the storage tank fluid. The system is then applied under the winter condition to find out the time for which the same air conditioners can be operated in a day. Hourly variations of solar insolation and ambient temperature for a particular day in April and January at Kolkata city in India have been considered for the calculation.

## **Chapter 2**

### **Methodology**

**Description of the system**

**Mathematical Modeling**

## Methodology

### 2.1 Description of the system

Solar thermal cooling system usually consists of a solar collector linked with an absorption chiller. The main components of the system are: solar collector, heat storage tank and absorption air-conditioning system. Heat is taken from the sun through the solar collector. From the solar collector, the absorbed heat is transferred to the storage tank through a circulating fluid, which is taken as water in this case. The storage material in the tank is also assumed to be water and the energy storage helps in the uninterrupted operation of the system. When the useful energy available from the sun ( $Q_u$ ) is more than the air-conditioning load ( $Q_g$ ), the extra energy gets stored in the storage tank. When the useful solar energy ( $Q_u$ ) is less than the required load ( $Q_g$ ), the deficit is made up by taking energy from the storage tank. A single-effect ammonia-water absorption air conditioning system is illustrated in Fig.19, where water is the absorbent and ammonia is the refrigerant. The four main parts of the basic absorption cycle are: the generator, the condenser, the evaporator and the absorber. There are other auxiliary components, like rectifier, expansion valve, heat exchanger and pump. Ammonia-water solution flows through these components with varying concentrations of ammonia (solute) in water (solvent).

The rich ammonia solution at high pressure is heated in the generator by using solar heat. Ammonia evaporates from the solution on heating, leaving the hot weak solution in the generator. High pressure ammonia vapor (state1) leaves the generator to enter the condenser, where the vapor condenses to high pressure saturated liquid ammonia (state2). The heat of condensation is rejected to the surrounding by supplying cooling water, which enters at ambient temperature. The liquid ammonia is then expanded through the expansion valve (state3) to reduce its pressure. As a result, the temperature of the refrigerant falls as well. The low pressure liquid is then evaporated in the evaporator section, by absorbing heat at low temperature. This gives the cooling effect in the system. After leaving the evaporator (state4), the low pressure ammonia vapor refrigerant enters the absorber, where it is absorbed by the cold weak solution. Thus the solution becomes rich again with ammonia. From the absorber the rich ammonia-water solution is pumped to the generator. The weak hot ammonia solution, which leaves the generator after the evaporation of ammonia, is passed through a heat exchanger (state: 8-9) where it transfers some heat to the rich solution. Then the weak solution comes back to the absorber by reducing its pressure in the expansion valve (state: 9-10).

The ammonia water cycle requires a rectifier, which is not shown in the figure, to purify the ammonia going into the refrigeration system from the generator. Without a rectifier, the ammonia vapor leaving the generator may contain some water vapor as well, which forms ice in the condenser. Formation

of ice blocks the expansion valve and freezes the pipeline. Moreover, water entering the evaporator lowers the cooling effect. The solution heat exchanger, as shown in the Fig. 19, is added to the system in order to improve the cycle performance. In the absorption air-conditioning cycle, the pump is the only part which requires work input. However this work input is much smaller than that required for the vapor compression refrigeration cycle. The remaining energy input, added in the generator, is taken from the sun.

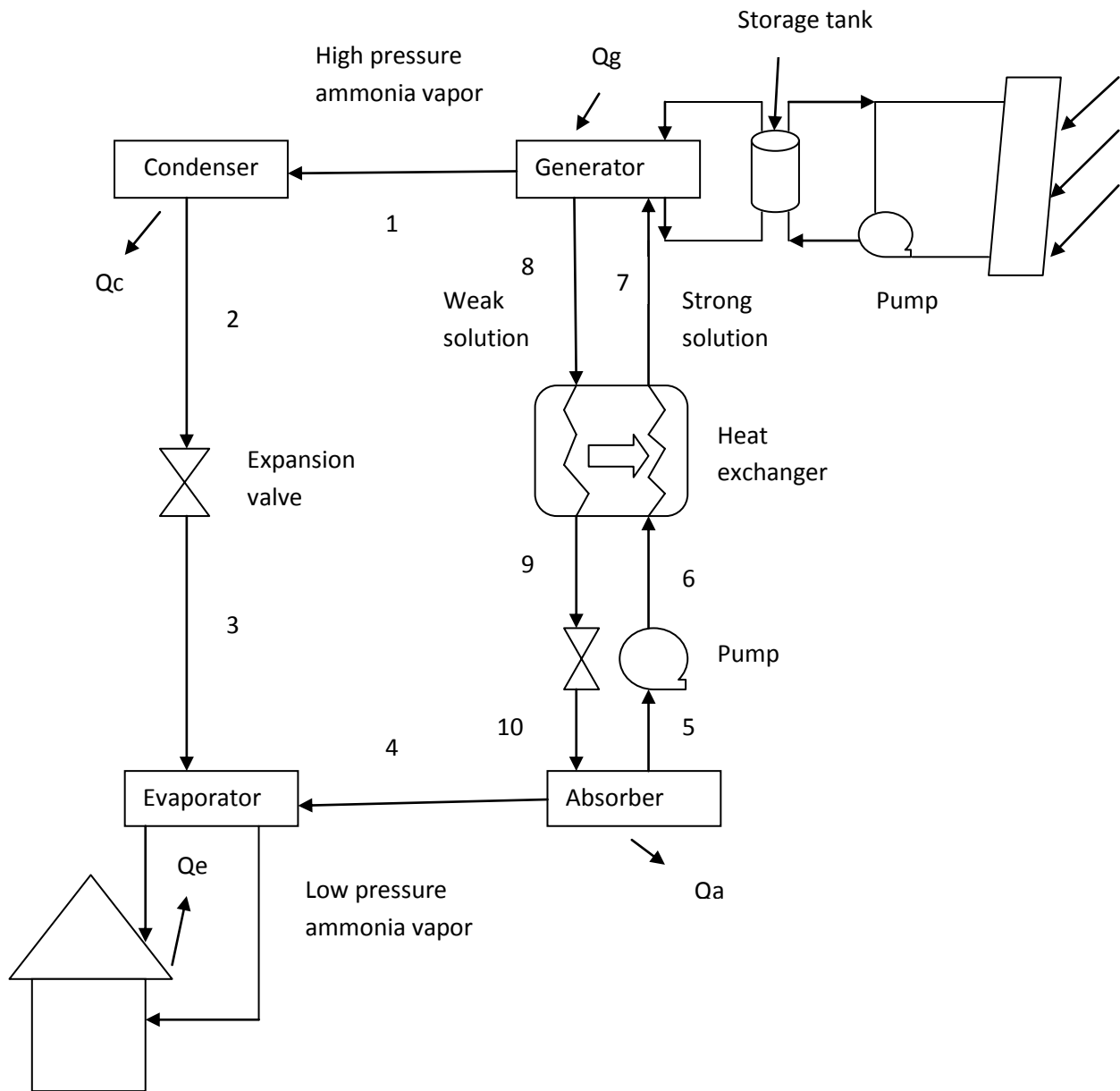


**Figure: 17 Schematic diagram of solar absorption air-conditioning system**

## 2.2 Mathematical Modeling

The necessary assumptions taken for modeling the system are as follows:

- The absorption refrigeration system working at two pressure levels  $P_h$  and  $P_l$ .
- Mass fraction of ammonia refrigerant flowing in the refrigeration cycle from state 1 to state 4 is 0.99 i.e.  $X=0.99$
- Mass flow rate of refrigerant  $\dot{m} = 1$  kg/min
- Liquid coming out from the condenser (at state 2), absorber (at state 5), and the weak solution from the generator (at state 8) are in their saturated state.
- The ammonia vapor from the evaporator is saturated (at state 4) and that from the generator is superheated (at state 1).
- The saturated liquid from the generator at state 8 loses heat to become sub-cooled at state 9 before entering the expansion valve.

The generator temperature ( $T_g$ ), condenser temperature ( $T_c$ ), evaporator temperature ( $T_e$ ) and absorber temperature ( $T_a$ ) are considered as the input parameters in the analysis. The pressure levels,  $P_h$  and  $P_l$ , are calculated from the temperature values using the relationship between saturated pressure  $P$  (Kpa), solution temperature  $T$  (K) and ammonia mass fraction  $X$  in the  $H_2O-NH_3$  mixture as [37]

$$\log P = A - \frac{B}{T} \quad (3)$$

$$A = 7.44 - 1.767X + 0.9823X^2 + 0.3627X^3 \quad (4)$$

$$B = 2013.8 - 2155.7X + 1540.9X^2 - 194.7X^3 \quad (5)$$

The thermodynamic property values at different state points are then calculated using suitable relations found in the literature. This has been elaborated in the following.

### State 1

The refrigerant (containing 99% ammonia and 1% water vapor) at state 1 has the pressure  $P_h$  and temperature  $T_g$ . The corresponding saturation temperature exists in the condenser ( $T_c$ ), where condensation takes place. The enthalpy of the vapor at state 1 is found using its relationship with mole fraction of ammonia in the vapor mixture ( $\bar{Y}$ ) and temperature at the given state as,

$$h_1 = h_{1sat} + C_{p,m}(T_g - T_c) \quad (6)$$

$$h_{1sat} = 1000 \sum_{i=1}^{17} a_i \left(1 - \frac{T}{324}\right)^{m_i} (1 - \bar{Y})^{n_i} / 4 \quad (7)$$

The coefficients  $a_i$ ,  $m_i$  and  $n_i$  in Eqn. (7) are taken from Sun [37] and are listed in the Appendix (Table A-1).

The molar specific heat of the saturated vapor mixture is calculated as follows [67]:

$$C_{p,m} = \bar{Y}C_{P,NH_3} + (1 - \bar{Y})C_{P,H_2O} \quad (8)$$

The molar specific heats of the saturated vapor of the two components are calculated using the equations

$$C_p(\tau) = A + B\tau^{-1/3} + C\tau^{-2/3} + D\tau^{-5/3} + E\tau^{-7.5/3} \quad (9)$$

where,  $\tau$  is represented using the vapor mixture temperature ( $T$ ) and the corresponding critical temperature ( $T_c$ ) as

$$\tau = 1 - \theta = 1 - \frac{T}{T_c} \quad (10)$$

$$\text{where, } T_c = \sum_{i=0}^4 b_i X^i \quad (11)$$

As evident from Eqn. (11), the critical temperature of the solution depends upon its composition and  $X$  is the mass fraction of ammonia in the liquid solution.

The parameters A to E in Eqn. (9) are obtained on the basis of IAPWS data (IAPWS 1997) [68], for water vapor, and from Haar & Gallagher (1978) [69] for ammonia. This equation is valid between the triple and critical points for pure substances [67].

Substance	A	B	C	D	E
NH <sub>3</sub>	-1.199197086	1.240129495	0.924818752	0.018199633	-0.245034 E-3
H <sub>2</sub> O	3.461825651	-4.987788063	2.994381770	6.259308 E-3	-8.262961 E-6

## **State 2**

The enthalpy of refrigerant coming from the condenser at state 2 is given as:

$$h_2(T, \bar{X}) = 100 \sum_{i=1}^{16} c_i \left(\frac{T}{273.16} - 1\right)^{p_i} \bar{X}^{q_i} \quad (12)$$

where,  $T$  and  $\bar{X}$  are the temperature and mole fraction of ammonia in the liquid solution at state 2.

Now the heat transfer rate in the condenser is:  $\dot{Q}_c = \dot{m}(h_1 - h_2)/60$  (13)

Since a throttling process has been used between state 2 and 3, the enthalpies at point 2 and at point 3 are equal, i.e.

$$h_2 = h_3 \quad (14)$$

The coefficient of Eqn. (12) is taken from **Sun [37]** and are listed in the Appendix (**Table A-2**).

#### **State 4**

The enthalpy of saturated refrigerant vapor, coming from evaporator, at state 4 is evaluated following Eqn. (7).

Heat transfer rate in the evaporator is given as:

$$\dot{Q}_e = \dot{m}(h_4 - h_3)/60 \quad (15)$$

#### **State 5**

After coming out from the evaporator at state 4 the ammonia (NH<sub>3</sub>) refrigerant gets absorbed by the weak liquid solution that comes from the generator to the absorber. From the absorber strong liquid solution comes out at state 5. The enthalpy of the liquid at state 5 is calculated following Eqn (12). To evaluate the enthalpy at state 5 it is necessary to calculate the mole fraction of ammonia in the strong liquid solution  $\bar{X}_{SS}$ .

The mole fraction of strong liquid solution  $\bar{X}_{SS}$  can be calculated as per the given equation:

$$T_l(P, \bar{X}) = 100 \sum_{i=1}^{14} d_i (1 - \bar{X}_{SS})^{r_i} \left[ \ln \left( \frac{2000}{P} \right) \right]^{s_i} \quad (16)$$

where, the constant terms are listed in the Appendix as **Table A-3**. Here  $T_l(P, \bar{X}) = T_a$ , and  $P = P_l$ . Thus, Eqn. (16) is solved to find out the value of  $\bar{X}_{SS}$ .

#### **State 6**

From state 5 to 6 the pump increases the pressure from  $P_l$  to  $P_h$ , and the required pump work is given as:

$$W_p = h_6 - h_5 = V_5(P_h - P_l) \quad (17)$$

Therefore, 
$$h_6 = h_5 + V_5(P_h - P_l) \quad (18)$$

The relation between specific volumes  $V_5$  ( $\text{m}^3/\text{Kg}$ ), temperature  $T$  ( $^{\circ}\text{C}$ ) and mass fraction  $X$  (decimal) of ammonia in saturated  $\text{H}_2\text{O}/\text{NH}_3$  solution is given as:

$$V_5(T, X) = \sum_{i=0}^3 \sum_{j=0}^3 e_{ij} X^j T^i \quad (19)$$

The coefficient of Eqn. (19) is taken from Sun [37] and are listed in the Appendix (Table A-4).

$T_6$  can be calculated from Eqn. 12 using the known values of  $h_6$  and  $\bar{X}_{ss}$ .

$$h_6(T, \bar{X}) = 100 \sum_{i=1}^{16} a_i \left( \frac{T}{273.16} - 1 \right)^{m_i} \bar{X}_{ss}^{n_i} \quad (20)$$

### State 8

The molar fraction of weak solution coming out from the generator at state 8 can be calculated following Eqn (16). Here  $P$  is replaced with  $P_h$  and  $\bar{X}_{ss}$  is replaced with  $\bar{X}_{ws}$ . The enthalpy at point 8 is calculated following Eqn. (12), where  $\bar{X}$  can be replace by  $\bar{X}_{ws}$  and  $T$  can be replaced with  $T_8$ .

### State 9

By losing heat through the heat exchanger the solution at state 9 become sub cooled liquid. The enthalpy at state 9 can be calculated as follows:

$$h_9 = h_8 - C_p(T_8 - T_9) \quad (21)$$

$T_9$  can be calculated from the energy balance of the heat exchanger and is given as:

$$T_9 = \epsilon T_6 + (1 - \epsilon)T_8 \quad (22)$$

where,  $\epsilon$  is the effectiveness of the heat exchanger and  $T_8 = T_9$ .

The specific heat of the saturated solution in the liquid phase ( $C_p$ ) can be calculated as follows:

$$C_p = \bar{X}_{ss} C_{p\text{NH}_3} + (1 - \bar{X}_{ss}) C_{p\text{H}_2\text{O}} \quad (23)$$

The specific heat of the saturated liquid of the two components are evaluated using the equation

$$C_p(\tau) = A_{cp} + B_{cp}(\tau^{-1}) \quad (24)$$



$\tau$  in above equation is calculated using Eqn. (10). The model parameters in the above equation are given as: [67]

substance	$A_{cp}$	$B_{cp}$
NH <sub>3</sub>	3.875648	0.242125
H <sub>2</sub> O	3.665785	0.236312

Since process 9 to 10 is a throttling process, specific enthalpy at state 9 and 10 are equal. Thus,

$$h_9 = h_{10} \quad (25)$$

Total mass balance in the generator gives,

$$\dot{m}_{ss} = \dot{m}_{ws} + \dot{m} \quad (26)$$

Total NH<sub>3</sub> balance in the generator gives,

$$\dot{m}X + \dot{m}_{ws}X_{ws} = \dot{m}_{ss}X_{ss} \quad (27)$$

It is assumed that,  $\dot{m} = 1 \text{ kg/min}$  and  $X = 0.99$

$X_{ws}$  and  $X_{ss}$  can be calculated from Eqn (16), thus  $\dot{m}_{ss}$  (mass flow rate of strong solution) and  $\dot{m}_{ws}$

(Mass flow rate of weak solution) are calculated from the above Eqns (26) and (27).

After calculating the mass flow rates of the strong and weak solutions, a parameter called circulation ratio, which the ratio of the mass flow rates of the weak absorbent solution and that of the refrigerant has been defined as,

$$f = \dot{m}_{ss}/\dot{m} \quad (28)$$

### **State 7**

The enthalpy at state 7 is calculated as follows,

$$h_7 = h_6 + \frac{\dot{m}_{ws}}{\dot{m}_{ss}}(h_8 - h_9) \quad (29)$$

Heat transfer rate to the system in the generator is given as,

$$\dot{Q}_g = (\dot{m}h_l + \dot{m}_{ws}h_8 - \dot{m}_{ss}h_7)/60 \quad (30)$$

Heat transfer rate in the absorber is given as,

$$\dot{Q}_a = (\dot{m}_{ws}h_{l0} + \dot{m}h_4 - \dot{m}_{ss}h_5)/60 \quad (31)$$

The coefficient of performance of the system can then be calculated as,

$$COP = \dot{Q}_e / (W_p + \dot{Q}_g) \quad (32)$$

In addition, energy loss to the environment takes place from the condenser and absorber and the rate of loss is the sum of  $\dot{Q}_c$  and  $\dot{Q}_a$ , as calculated from Eqns. (13) and (30).

#### CALCULATION OF SOLAR COLLECTOR AND STORAGE SYSTEM

The design of the solar collector and storage system has also been performed using the global horizontal irradiance ( $E$ ) and direct normal irradiance ( $E_{bn}$ ) taken from meteorological solar insolation data of Kolkata.

$$\text{Now,} \quad E = E_{bn} \cos \theta_z + E_d \quad (33)$$

Here,  $E_d$ =hourly diffused radiation data and  $\theta_z$  is the solar zenith angle. The latter is calculated as,

$$\cos \theta_z = \sin \varphi \sin \delta + \cos \varphi \cos \delta \cos \omega \quad (34)$$

where,  $\varphi$ = latitude of the location, i.e. the angle made by the radial line joining the location to the centre of the earth with the projection of the line on the equatorial plane.

$\delta$  = angle made by the line joining the centre of sun and the earth with its projection on the equilateral plane.

$$\delta = 23.45 \sin\left[\frac{360}{365}(284 + n)\right] \quad (35)$$

n= number of days

$\omega$  is the hour angle which is an angular measure of time and is equivalent to  $15^\circ$  per hour. It also varies from  $-180^\circ$  to  $+180^\circ$ . We adopt the convention of measuring it from noon based on local apparent time (LAT), being positive in the morning and negative in the afternoon.

The evacuated tube collector is placed facing south with a tilt angle  $\beta = 15^\circ$ . Thus, the solar azimuth angle  $\gamma = 0$ . Thus, the solar radiation ( $E_s$ ) incident on the titled collector surface with contributions from beam, diffuse and ground reflected radiations is given as,

$$E_s = E_b r_b + E_d r_d + (E_b + E_d) r_r \quad (36)$$

$r_b$  is the tilt factor for beam radiation. It is the ratio of the beam radiation flux falling on a tilted surface to that falling on a horizontal surface.

$$r_b = \frac{\cos \theta}{\cos \theta_z} = \frac{\sin \delta \sin(\varphi - \beta) + \cos \delta \cos \omega \cos(\varphi - \beta)}{\sin \varphi \sin \delta + \cos \varphi \cos \delta \cos \omega} \quad (37)$$

Where,  $\beta$  is a tilted angle and  $\theta$  is the angle of incident.

Now the tilt factor for diffused radiation is given as,

$$r_d = \frac{1 + \cos \beta}{2} \quad (38)$$

Tilt factor for ground reflected radiation is given as,

$$r_r = \rho \left( \frac{1 - \cos \beta}{2} \right) \quad (39)$$

Where  $\rho$  is the ground reflectivity and its value is taken as 0.2 [70].

We have used evacuated tube selective surface solar collector to capture the solar insolation. The solar collector efficiency can be calculated as,

$$\epsilon_c = F_R \left( \tau \alpha - U_l \left( \frac{T_i - T_a}{E_s} \right) \right) \quad (40)$$

Where,  $F_R$  = collector heat removal factor

$\tau$  = transmissivity of the glass cover system, it is the ratio of the solar radiation coming through after reflection at the glass-air interfaces and absorption in the glass to the radiation incident on the glass cover system.

$\alpha$  = absorptivity of the absorber plate

$U_l$  = overall loss coefficient

$T_i$  = water inlet temperature to the solar collector

$T_a$ = hourly variation ambient temperature taken from meteorological data

The parameter of evacuated tube collector have been selected as,  $F_R(\alpha\tau)=0.7$  [71] and  $F_R U_L=3.3$  [71].

The useful energy collected from the solar insolation through solar collector is given by,

$$\dot{Q}_u = A_c E_s \epsilon_c \quad (41)$$

$A_c$ = required collector area

$\epsilon_c$ = collector efficiency

Here we have used storage tank to store the excess energy that is collected through the solar collector. When the useful energy ( $\dot{Q}_u$ ) is more than the generator load  $\dot{Q}_g$ , the extra energy is stored in the storage tank. On the other hand, when the useful energy is less than the generator load  $\dot{Q}_g$ , the necessary extra energy is taken from the storage tank.

Due to energy exchange across the storage tank, the storage tank temperature varies. As, water is considered as the storage material, the temperature of water needs to be monitored with time to ensure that it remains below the boiling point temperature. The variation of the storage tank temperature with time is given by the equation,

$$\frac{\dot{Q}_u - \dot{Q}_g - (UA)(T_l - T_a)}{\dot{Q}_u - \dot{Q}_g - (UA)(T_{li} - T_a)} = \exp \left[ - \frac{(UA)t}{(\rho V C_p)} \right] \quad (42)$$

In the above equation,  $U$ = average overall heat transfer coefficient for heat loss from the tank = 0.72 W/m<sup>2</sup> K [71]

$A$ = heat transfer surface area of storage tank considered to be of cubic shape

$T_{li}$ = initial temperature of storage tank

$\dot{Q}_u$ = useful heat captured by solar collector

$\rho V$ = mass of storage medium in the tank, which has been calculated considering a value of mass per unit collector area=75 kg/m<sup>2</sup> [71].

$\dot{Q}_g$ = generator load, which is the amount of heat absorbed in the generator of absorption refrigeration system for operating 10 numbers of 2 ton air conditioner.

Now we know that 1 ton refrigeration is equivalent to energy removal at a rate of 3.5 kW in the evaporator. Thus, the total cooling load in the evaporator  $\dot{Q}_e=70$  kW

The solar air conditioner system is designed to operate with parameters corresponding to the maximum COP as evaluated for the absorption refrigeration cycle. The corresponding parameters are,

$$T_g = 90^\circ\text{C}, T_c = 20^\circ\text{C}, T_e = 7.5^\circ\text{C}, T_a = 25^\circ\text{C}$$

From the value of the computed COP for the above operating parameters, the generator load,  $\dot{Q}_g$ , can be calculated using Eqn. (31).

Now from meteorological data and required heating load of the entire system ( $Q_g$ ) the variation of storage tank temperature of the whole day and required collector area to drive this load is calculated using Eqn. (41). Using Eqn. (41) we have evaluate the hourly variation of storage tank temperature for the whole day. We have seen that the temperature of storage tank in a specific day at morning at 7.00 a.m is coinciding with the temperature to the next day at morning at 7.00 a.m. This indicate that there is an matching between the useful heat gain and the energy withdrawn over a day and the purpose of storage tank to take care of the short term mismatch between supply and demand of energy over a day is fulfilled.

## **Chapter 3**

### **Result and discussion**

#### **3.1 Performance evaluation of absorption refrigeration system under different parametric conditions**

##### **3.1.1 Effect of generator temperature ( $T_g$ )**

##### **3.1.2 Effect of absorber temperature ( $T_a$ )**

##### **3.1.3 Effect of condenser temperature ( $T_c$ )**

##### **3.1.4 Effect of evaporator temperature ( $T_e$ )**

#### **3.2 Design calculation of solar powered vapor absorption air-conditioning system**

### 3.1 Performance evaluation of absorption refrigeration system under different parametric conditions

Here the performances of absorption refrigeration cycle at different parametric conditions have been studied. A modular software programme has been developed to calculate the coefficient of performance of the system by varying the various parametric conditions such as  $T_g = 60^\circ\text{C}$  to  $90^\circ\text{C}$ ,  $T_c = 20^\circ\text{C}$  to  $40^\circ\text{C}$ ,  $T_e = -5^\circ\text{C}$  to  $7.5^\circ\text{C}$ ,  $T_a = 20^\circ\text{C}$  to  $40^\circ\text{C}$ . From the above study optimum COP is chosen to drive the absorption cooling system at this condition i.e.  $T_g = 90^\circ\text{C}$ ,  $T_e = 7.5^\circ\text{C}$ ,  $T_c = 20^\circ\text{C}$ ,  $T_a = 25^\circ\text{C}$  linked with solar collector and water storage system.

#### 3.1.1 Effect of generator temperature ( $T_g$ )

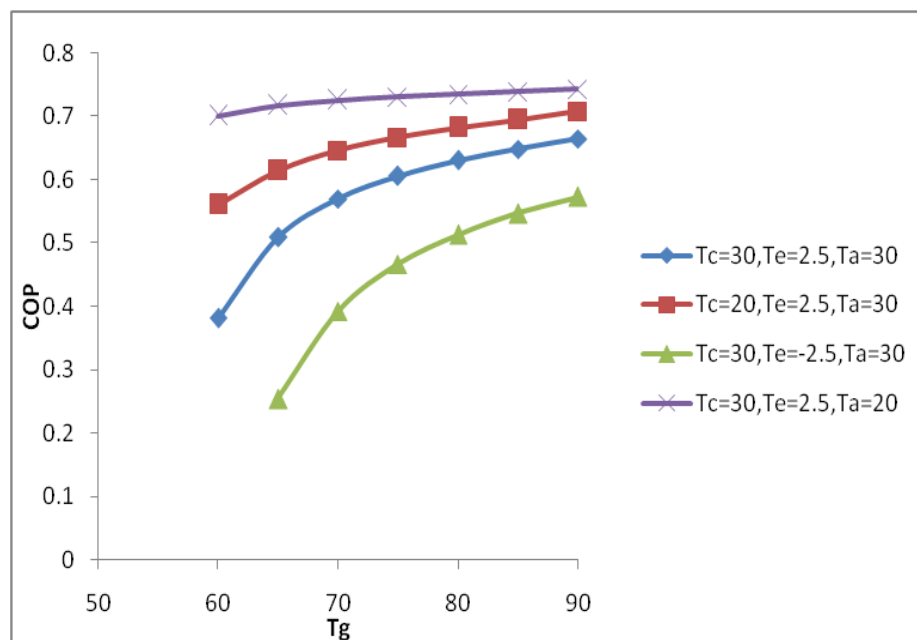


**Figure: 18 (a) Variation of coefficient of performance (COP) with generator temperature ( $T_g$ )**

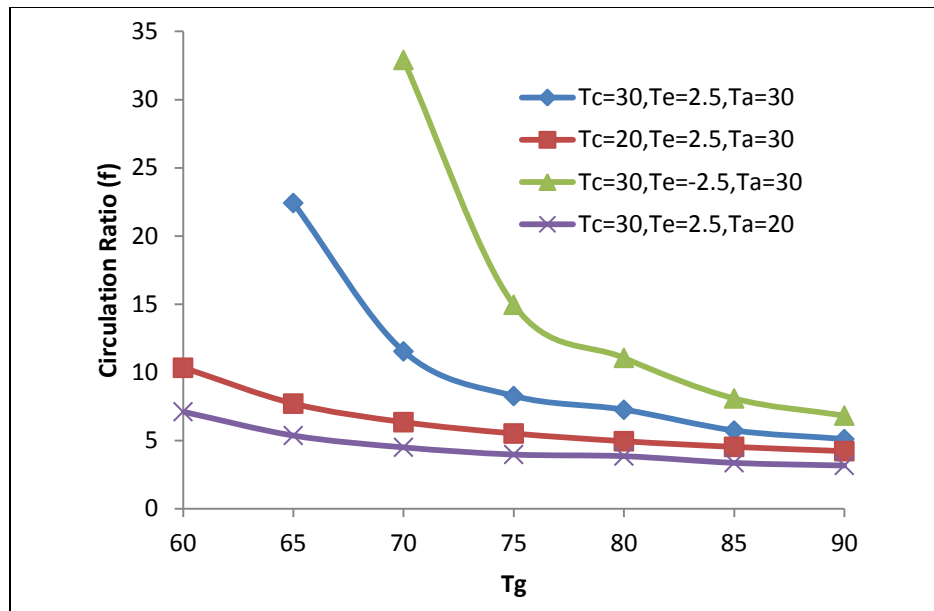


**Figure: 18 (b) Variation of circulation ratio with generator temperature ( $T_g$ )**

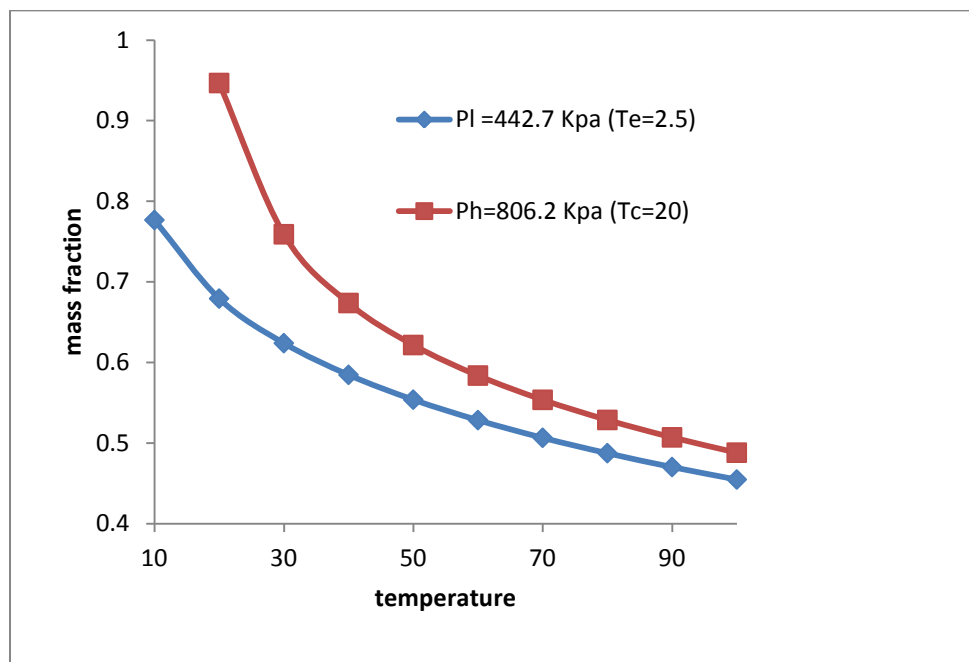


**Figure: 19 Variation of mass fractions with temperature**

The variation of system coefficient of performance with generator temperature is shown in Fig. 18 (a). As we can see from the Fig. 18(a) that for generator temperature range between 60°C to 90°C the coefficient of performance varies between 0.25 to 0.75, for different parametric conditions i.e. condenser temperature, evaporator temperature and absorber temperature. At a given  $T_c$ ,  $T_e$  and  $T_a$ , the coefficient of



performance increases with increasing generator temperature. This is primarily because with the increase of generator temperature the heat input to the generator  $Q_g$  decreases. It can be shown from Eqn. (26) and Eqn. (27) that,

$$\frac{\dot{m}}{\dot{m}_{ss}} = 1 - (X - X_{ss}) / (X - X_{ws}) \quad (43)$$

$\frac{\dot{m}}{\dot{m}_{ss}}$  is the inverse of the circulation ratio. It is seen from Fig. 21 that mass fraction of ammonia decreases with temperature. Thus in this case as the generator temperature increases  $X_{ws}$  decreases. However as the absorber temperature remains constant  $X_{ss}$  also remains constant. Thus with the increase of generator temperature  $\frac{\dot{m}}{\dot{m}_{ss}}$  increases following Eqn. 42, thus decreasing the circulation ratio.

The refrigerant mass flow rate  $\dot{m}$  has been kept constant under all conditions. Thus circulation ratio decreases only because of the decrement of  $\dot{m}_{ss}$ . When  $\dot{m}_{ss}$  is reduced at higher generator temperature, the rate of heat absorption ( $Q_g$ ) in the generator get decreases. This increases the COP. For the parametric condition i.e.  $T_c = 30^\circ\text{C}$ ,  $T_e = 2.5^\circ\text{C}$ ,  $T_a = 20^\circ\text{C}$  the increment of COP with generator temperature as shown in Fig. 18(a) and the decrement of circulation ratio shown in Fig. 18 (b) is very slow almost tends to be constant.

### 3.1.2 Effect of absorber temperature ( $T_a$ )

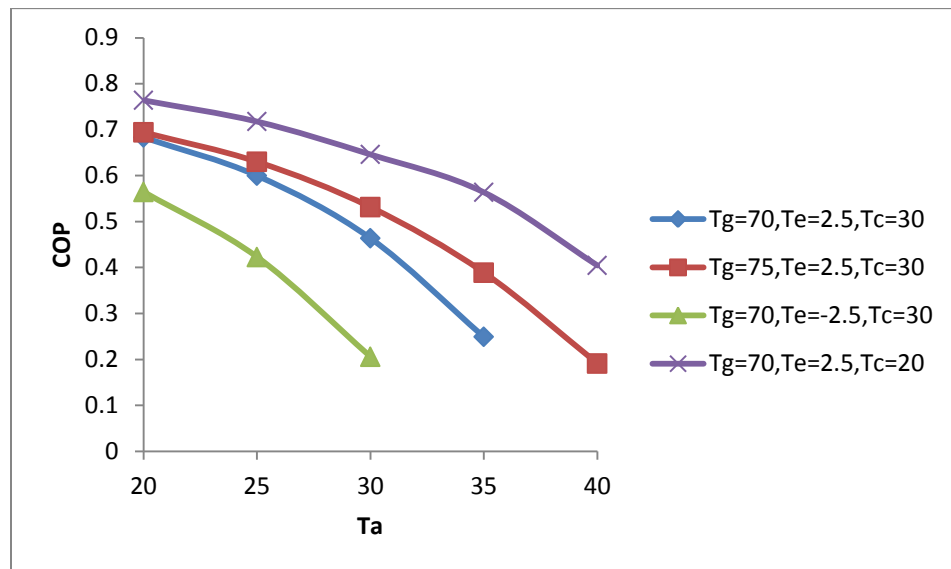
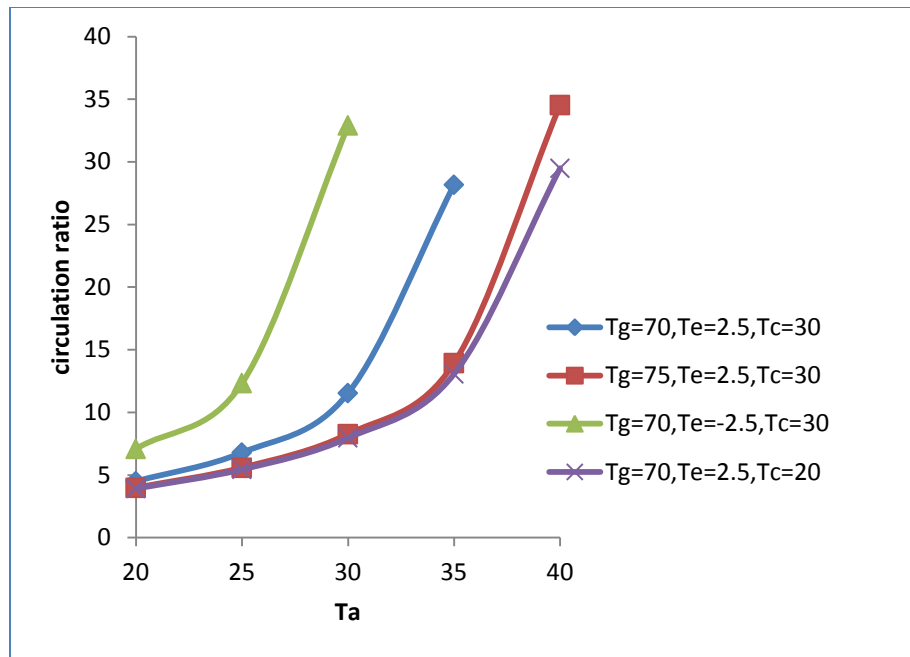


Figure: 20 (a) variation of coefficient of performance (COP) with absorber temperature ( $T_a$ )



**Figure: 20 (b) Variation of circulation ratio with absorber temperature ( $T_a$ )**

The variation of system coefficient of performance with absorber temperature is shown in Fig 20 (a). As we have seen from the above Fig. 20 (a) that for absorber temperature range between 20°C to 40°C the coefficient of performance varies from 0.1911 to 0.7641 for different parametric condition  $T_g$  (generator temperature),  $T_e$  (evaporator temperature),  $T_c$  (condenser temperature). For a given  $T_g, T_e, T_c$  the coefficient of performance decreases with absorber temperature. It is seen from Fig. 19 that mass fraction of ammonia decreases with temperature. Thus in this case as the absorber temperature increases  $X_{ss}$  decreases. However as the generator temperature remains constant,  $X_{ws}$  also remains constant. Thus with the increase of absorber temperature  $\frac{\dot{m}}{\dot{m}_{ss}}$  is decreased following Eqn. 42. Since  $\frac{\dot{m}}{\dot{m}_{ss}}$  is the inverse of circulation ratio, thus with the increase of absorber temperature circulation ratio will increase. As the refrigerant mass flow rate remains constant under all conditions, thus with the increase of absorber temperature mass flow rate of strong solution ( $\dot{m}_{ss}$ ) increases. Since  $\dot{m}_{ss}$  increases with absorber temperature, more heat is absorbed in the generator, increasing  $Q_g$ . With the increase of  $Q_g$ , COP get decreases. It is also observed during the study that the cycle could not be operated over the whole range of absorber temperature considered for all the chosen values of the other three temperatures. For example, when  $T_g = 70^\circ\text{C}, T_e = -2.5^\circ\text{C}, T_c = 30^\circ\text{C}$ , the cycle performance only gives realistic values up to an absorber temperature of 30°C. On the other hand, for  $T_g = 70^\circ\text{C}, T_e = 2.5^\circ\text{C}, T_c = 30^\circ\text{C}$ , realistic performance of the cycle could only be achieved up to  $T_a = 35^\circ\text{C}$ . These indicate that the absorber

temperature in the system has got a limit of operation depending upon the other cycle parameters existing in the system.

### 3.1.3 Effect of condenser temperature ( $T_c$ )

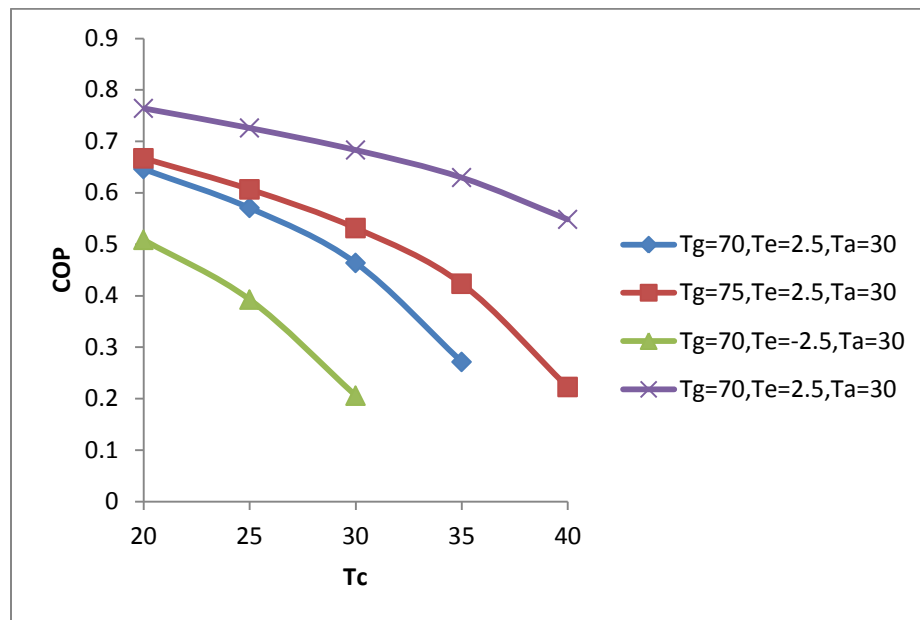


**Figure: 21** variation of coefficient of performance (COP) with condenser temperature ( $T_c$ )

A more detailed study on the effect of variation in condenser temperature is shown in Fig. 21. As we have seen from the figure that for condenser temperature range between  $20^\circ\text{C}$  to  $40^\circ\text{C}$  the coefficient of performance varies from 0.206 to 0.764 for different parametric condition  $T_g$  (generator temperature),  $T_e$  (evaporator temperature),  $T_a$  (absorber temperature). For a given  $T_g$ ,  $T_e$ ,  $T_a$  coefficient of performance decreases with the increase condenser temperature. It can be shown for a reversible Carnot refrigerator that the performance of the device improves with the increase in the low temperature reservoir and the decrease in the high temperature reservoir. Here, the temperature of the evaporator represents the temperature of the low temperature reservoir as the heat is taken from the load into the evaporator. On the other hand, condenser temperature represents the high temperature reservoir, at which the heat is rejected into the environment. The present results clearly show that the variation in performance of the cycle is in line with the reversible cycle, qualitatively.

### 3.1.4 Effect of evaporator temperature ( $T_e$ )

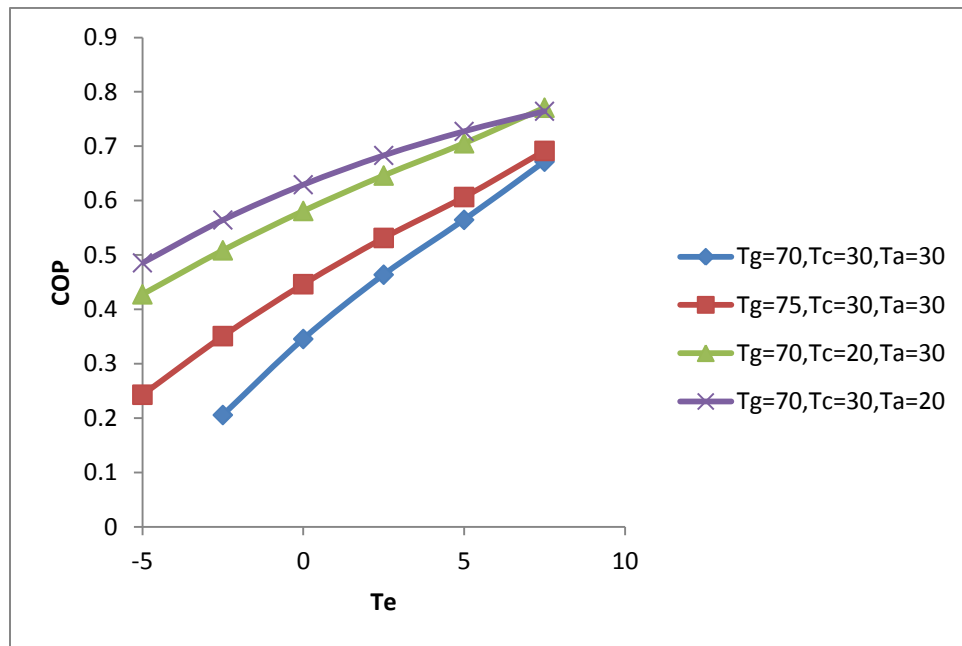


**Figure: 22** variation of coefficient of performance (COP) with evaporator temperature ( $T_e$ )

The variation of system coefficient of performance with evaporator temperature is shown in Fig 22. As we can see from the above figure that for evaporator temperature range between  $-5^{\circ}\text{C}$  to  $7.5^{\circ}\text{C}$  the coefficient of performance varies from 0.2 to 0.77 for different parametric condition i.e.  $T_c$  (condenser temperature),  $T_g$  (generator temperature),  $T_e$  (evaporator temperature). For a given  $T_g$ ,  $T_c$ ,  $T_a$  the coefficient of performance improve with evaporator temperature. It can be shown for a reversible Carnot refrigerator that the performance of the device improves with the increase in the low temperature reservoir and the decrease in the high temperature reservoir. Here, the temperature of the evaporator represents the temperature of the low temperature reservoir as the heat is taken from the load into the evaporator. On the other hand, condenser temperature represents the high temperature reservoir, at which the heat is rejected into the environment. The present results clearly show that the variation in performance of the cycle is in line with the reversible cycle, qualitatively. Since the cooling load of the system improves with evaporator temperature, the system efficiency i.e. the coefficient of performance automatically improves. For a parametric condition  $T_g = 70^{\circ}\text{C}$ ,  $T_c = 30^{\circ}\text{C}$ ,  $T_a = 30^{\circ}\text{C}$  there is an unrealistic value for  $T_e = -5^{\circ}\text{C}$ , thus this value is not considered here. This indicates that in this condition the absorption refrigeration system will not operate.

### 3.2 Design calculation of solar powered vapor absorption air-conditioning system

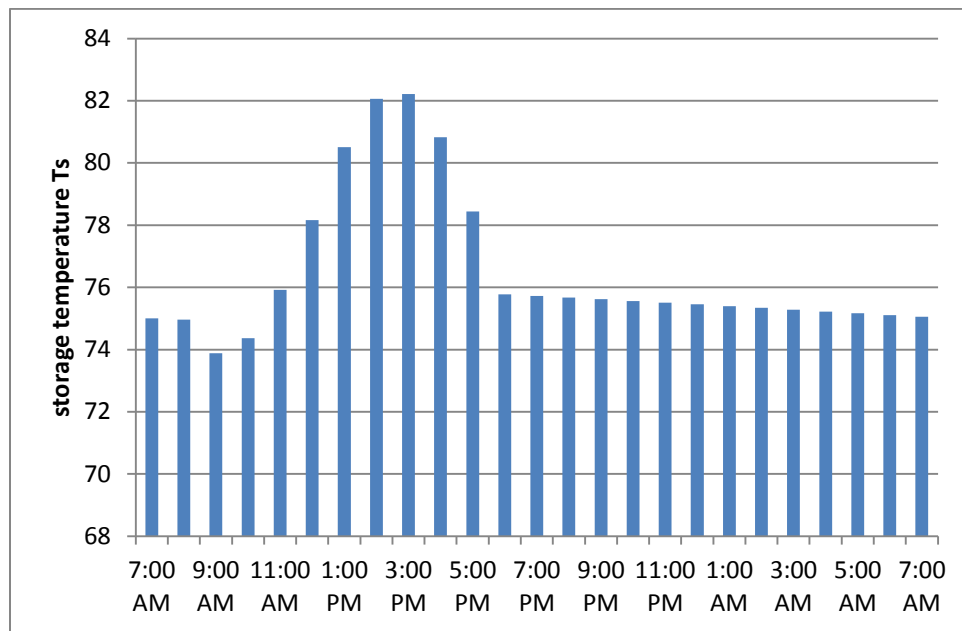


Figure: 23 Hourly variation of storage tank temperature ( $T_s$ ) for summer month

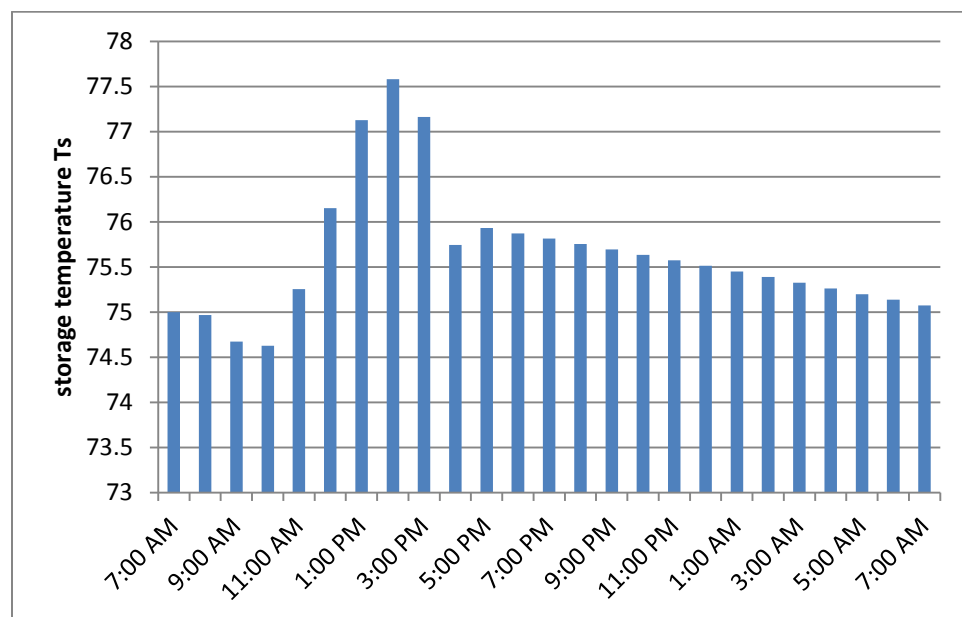


Figure: 24 Hourly variation of storage tank temperature ( $T_s$ ) for winter month

In this thesis we have designed a solar powered vapor absorption air-conditioning system. For this purpose we have considered 10 numbers of 2 ton air-conditioning system for an office space in Kolkata, India. Since the system is driven by solar power, we have chosen an evacuated tube collector as a collecting device. The advantages of using evacuated tube collector as a collecting device have already been elaborated in Section 1.3.7. A storage tank has been taken into consideration for a uninterrupted operation of the plant under daily and seasonal variations of solar insolation.

The purpose of the design is to calculate the collector surface area and the variation in the temperature of the storage material with time. The meteorological data of the summer season has been considered for the design as they are more extreme in a year. Thus, using the summer data of solar insolation and ambient temperature, the collector surface area and variation of storage tank temperature are calculated to operate the air-conditioning load for 10 hours in a day. Later the same area has been used to calculate the duration of operation of the system in case of winter season by using the corresponding meteorological data.

We have used solar insolation data and ambient temperature data for the months of April (as summer) and January (as winter), which are listed in the Appendix (**Table-A5, Table-A6, Table-A7, Table-A8, Table-A9, Table-A10**). Observing the data we can say that the values of solar insolation and ambient temperature are low in case of winter month than those of summer month. The value of solar insolation is low at the start of the day; it gradually increases up to noon and touches the peak at 12o'clock; after that it decreases up to 4 p.m. The same type of variations have been seen in case of ambient temperature data, after 12o'clock the ambient temperature gradually decreases till the next day.

Figure 24 represent the hourly variation of storage tank temperature for a specific day from 7.00 a.m to the next day at 7.00 a.m for a month of summer. We have chosen the initial temperature of the storage tank as 75°C. During choosing the initial temperature of storage tank we should keep in mind that the maximum peak temperature attained by the storage material should be lower than the boiling point temperature of the storage material, in this case water. It is seen from Fig. 24 that from 7.00 a.m to 9.00 a.m the storage tank temperature decreases, this is because at that time duration the solar insolation is low. Thus the useful heat gain will also be low i.e. the energy withdrawn from the system ( $\dot{Q}_g$ ) exceed the useful heat gain ( $\dot{Q}_u$ ). Thereafter the solar insolation start increasing up to 12 p.m, thus the useful heat gain also increases. At the time duration between 10 a.m to 3 p.m the useful energy ( $\dot{Q}_u$ ) exceed the load demand ( $\dot{Q}_g$ ) and excess energy store in the storage tank, thus the storage material temperature also increases at this time duration and touches the peak at 2.00 p.m. The highest temperature attain by the storage tank is 82°C , after that storage tank temperature decreases. This is because of the fact that at 4.00

p.m the solar insolation decreases suddenly to a very low value, at the time duration 4.00 p.m to 5 p.m the load demand exceed the useful heat gain thus storage tank temperature decreases suddenly. After 5.00 p.m both load demand and useful heat gain become absent, still storage tank temperature decreases very slowly due to thermal losses.

In winter (Fig. 25) the same type of variation in the storage temperature is observed, but the difference is that due to lower solar insolation the peak temperature attained by the storage material is 77.5°C which is much lower than boiling point temperature of storage material. Both in case of summer and winter if we take the lower mass of water as a storage material, the storage tank temperature attain higher peak value, but in that case there is a risk of attaining boiling point temperature i.e. 100°C , which is not desirable.

We have assumed that in summer season the 10 numbers of 2 ton air-conditioning systems will operate 10 hour in a day in office space at Kolkata. To operate such system at that time duration the required collector surface area is 372 m<sup>2</sup>. By using this collector area we have also calculated the duration of operation of the system during winter season in a single day, it becomes 8 hour.

## **Chapter 4**

### **Conclusion**

### **Scope of future work**



## 4.1 Conclusion

Design of solar powered absorption air-conditioning system has been analyzed in this work. Solar absorption air-conditioning system usually consists of solar collector linked with absorption air-conditioning system. The main components of such system are: solar collector, a heat storage tank and an absorption cooling system. We have used evacuated tube collector for collecting the solar irradiance. Due to higher efficiency and lower convective losses evacuated tube collector is used. The main components of absorption cooling system are: generator, condenser, evaporator and absorber. The auxiliary components are: expansion valve, solution heat exchanger and pump. Heat is taken from the sun through solar collector. The useful heat collected by the solar collector is transfer to the storage tank. These transfer heat withdrawn by the generator of the air-conditioning system. The absorption cooling system operates for 10 numbers of 2 ton air-conditioning systems i.e. produce a cooling load of 70 KW. The air-conditioning system will operate for 10 hour a day in summer month and 8 hour a day in winter month.

The following conclusion can be drawn from the study. The total numerical design is done in MATLAB 8.1 software. By software programming we have evaluated the coefficient of performance by varying various parametric condition i.e. generator temperature, evaporator temperature, absorber temperature and condenser temperature. It seen that the coefficient of performance increases with generator and evaporator temperature and decreases with condenser and absorber temperature. Among the ranges of input parameters chosen, the maximum COP is evaluated as 0.8262. The optimum parametric condition for this COP value is  $T_g = 90^\circ\text{C}$ ,  $T_e = 7.5^\circ\text{C}$ ,  $T_c = 20^\circ\text{C}$ ,  $T_a = 25^\circ\text{C}$ . To drive the entire system at this parametric condition the required collector area for summer month is  $372 \text{ m}^2$ , the same has been used for winter month. But in winter the system will operate for 8 hour instead of 10 hour. From the analysis it is concluded that the coefficient of performance of the system will increase with generator and evaporator temperature and decrease with condenser and absorber temperature. Also the storage tank temperature variation calculate through the modular computer programme and it is seen that at summer storage tank temperature will reach the peak value is  $82^\circ\text{C}$  where as for winter it is reached at  $77.5^\circ\text{C}$ . It is analyzed from the data that after the whole day the storage tank temperature will match with its initial temperature. This indicates that the storage tank is serving its purpose of handling the short term mismatch between useful energy and load demand over a day.

## 4.2 Scope of future work

The present work has been analyzed the performance of single effect solar driven absorption air-conditioning system with  $\text{NH}_3\text{-H}_2\text{O}$  as a working fluid. This work may be extended further with the aim of making the system more efficient.

- 1) Exergy analysis of the same system can be done.
- 2) The same thermodynamical analysis can be done for double effect absorption cooling system.
- 3) Other working fluid can be used for the same system such as  $\text{H}_2\text{O-LiBr}$ ,  $\text{NH}_3\text{-NaSCN}$  etc.
- 4) Modification can be done in case of solar collector also; we can use concentrating solar collector instead of evacuated tube collector.

**Appendix**Table-A-1: Value of coefficient  $i$ ,  $m_i$ ,  $n_i$ ,  $a_i$  regarding Eqn. (7)

$i$	$m_i$	$n_i$	$a_i$	$i$	$m_i$	$n_i$	$a_i$
1	0	0	1.28827	9	0	3	-6.70515
2	1	0	$1.25247 \cdot 10^{-1}$	10	1	3	$1.64508 \cdot 10^1$
3	2	0	-2.08748	11	2	3	-9.36849
4	3	0	2.17696	12	0	4	8.42254
5	0	2	2.35687	13	1	4	-8.58807
6	1	2	-8.86987	14	0	5	-2.77049
7	2	2	$1.02635 \cdot 10^1$	15	4	6	$-9.61248 \cdot 10^{-1}$
8	3	2	-2.3744	16	2	7	$9.88009 \cdot 10^{-1}$
				17	1	10	$3.08482 \cdot 10^{-1}$

Table-A-2: Value of coefficient  $i$ ,  $p_i$ ,  $q_i$ ,  $c_i$  regarding Eqn. (12)

$i$	$p_i$	$q_i$	$c_i$	$i$	$p_i$	$q_i$	$c_i$
1	0	1	-7.6108	9	2	1	2.84179
2	0	4	$2.56906 \cdot 10^1$	10	3	3	7.41609
3	0	8	$-2.47092 \cdot 10^2$	11	5	3	$8.91844 \cdot 10^2$
4	0	9	$3.25952 \cdot 10^2$	12	5	4	$-1.61309 \cdot 10^3$
5	0	12	$-1.58854 \cdot 10^2$	13	5	5	$6.22106 \cdot 10^2$
6	0	14	$6.19084 \cdot 10^1$	14	6	2	$-2.07588 \cdot 10^2$
7	1	0	$1.14314 \cdot 10^1$	15	6	4	-6.87393
8	1	1	1.18157	16	8	0	3.50716

Table-A3: Value of coefficient  $i$ ,  $r_i$ ,  $s_i$ ,  $d_i$  regarding Eqn. (16)

$i$	$r_i$	$s_i$	$d_i$	$i$	$r_i$	$s_i$	$d_i$
1	0	0	3.22302	8	1	2	$1.06154 \cdot 10^{-2}$
2	0	1	$-3.84206 \cdot 10^{-1}$	9	2	3	$-5.33589 \cdot 10^{-4}$
3	0	2	$4.60965 \cdot 10^{-2}$	10	4	0	7.85041
4	0	3	$-3.78945 \cdot 10^{-3}$	11	5	0	$-1.15941 \cdot 10^{-1}$
5	0	4	$1.3561 \cdot 10^{-4}$	12	5	1	$-5.2315 \cdot 10^{-2}$
6	1	0	$4.87755 \cdot 10^{-1}$	13	6	0	4.89596
7	1	1	$-1.20108 \cdot 10^{-1}$	14	13	1	$4.21059 \cdot 10^{-2}$

Table-A4: Value of coefficient  $i$ ,  $j$ ,  $e_{ij}$  regarding Eqn. (19)

$i$	$j$	$e_{ij}$	$i$	$j$	$e_{ij}$
0	0	$9.9842 \cdot 10^{-4}$	0	2	$-1.2006 \cdot 10^{-4}$
1	0	$-7.8161 \cdot 10^{-8}$	1	2	$1.0567 \cdot 10^{-5}$
2	0	$8.7601 \cdot 10^{-9}$	2	2	$2.4056 \cdot 10^{-7}$
3	0	$-3.9076 \cdot 10^{-11}$	3	2	$1.9851 \cdot 10^{-9}$
0	1	$3.5489 \cdot 10^{-4}$	0	3	$3.2426 \cdot 10^{-4}$
1	1	$5.2261 \cdot 10^{-6}$	1	3	$9.8890 \cdot 10^{-6}$
2	1	$-8.4137 \cdot 10^{-8}$	2	3	$-1.87158 \cdot 10^{-7}$
3	1	$6.4816 \cdot 10^{-10}$	3	3	$1.7727 \cdot 10^{-9}$

Table-A5: Variation of global horizontal irradiance with time over a day in January at Kolkata[72]

hour	Global horizontal data ( $I_g$ ) in $W/m^2$
7.00 a.m	136
8.00 a.m	311
9.00 a.m	475
10.00 a.m	594
11.00 a.m	639
12.00 p.m	653
1.00 p.m	555
2.00 p.m	403
3.00 p.m	227
4.00 p.m	49

Table-A6: Variation of direct normal irradiance with time over a day in January at Kolkata[72]

hour	Direct normal radiation ( $I_{bn}$ ) in $w/m^2$
7.00 a.m	60
8.00 a.m	240
9.00 a.m	364
10.00 a.m	442
11.00 a.m	475
12.00 p.m	480
1.00 p.m	444
2.00 p.m	318
3.00 p.m	172
4.00 p.m	6

Table-A7: Variation of ambient temperature with time over a day in January at Kolkata[72]

hour	Ambient temperature ( $T_a$ ) in °C	hour	Ambient temperature ( $T_a$ ) in °C
7.00 a.m	14.6943	7.00 p.m	17.5772
8.00 a.m	19.231	8.00 p.m	17.193
9.00 a.m	22.5534	9.00 p.m	16.8699
10.00 a.m	24.5774	10.00 p.m	16.5675
11.00 a.m	25.8913	11.00 p.m	16.1753
12.00 p.m	26.4901	12.00 p.m	14.2171
1.00 p.m	26.4771	1.00 a.m	14.1151
2.00 p.m	25.0565	2.00 a.m	14.0689
3.00 p.m	22.6795	3.00 a.m	13.6873
4.00 p.m	19.6285	4.00 a.m	13.281
5.00 p.m	18.7437	5.00 a.m	12.8147
6.00 p.m	18.0583	6.00 a.m	12.6184

Table-A8: Variation of global horizontal irradiance with time over a day in April at Kolkata[72]

hour	Global horizontal data ( $I_g$ ) in $W/m^2$
7.00 a.m	210
8.00 a.m	379
9.00 a.m	557
10.00 a.m	693
11.00 a.m	751
12.00 p.m	762
1.00 p.m	666
2.00 p.m	516
3.00 p.m	324
4.00 p.m	215

Table-A9: Variation of direct normal irradiance with time over a day in April at Kolkata[72]

hour	Direct normal radiation ( $I_{bn}$ ) in $w/m^2$
7.00 a.m	197
8.00 a.m	347
9.00 a.m	474
10.00 a.m	569
11.00 a.m	589
12.00 p.m	596
1.00 p.m	546
2.00 p.m	476
3.00 p.m	318
4.00 p.m	123

Table-A10: Variation of ambient temperature with time over a day in April at Kolkata[72]

hour	Ambient temperature ( $T_a$ ) in °C	hour	Ambient temperature ( $T_a$ ) in °C
7.00 a.m	23.3835	7.00 p.m	23.9038
8.00 a.m	29.073	8.00 p.m	23.1481
9.00 a.m	32.2574	9.00 p.m	22.5244
10.00 a.m	34.2408	10.00 p.m	22.0274
11.00 a.m	35.4637	11.00 p.m	21.6602
12.00 p.m	35.9254	12.00 p.m	19.7783
1.00 p.m	35.4095	1.00 a.m	19.4961
2.00 p.m	33.9202	2.00 a.m	19.1295
3.00 p.m	31.5933	3.00 a.m	18.6706
4.00 p.m	28.102	4.00 a.m	18.0942
5.00 p.m	25.9699	5.00 a.m	17.5912
6.00 p.m	24.8852	6.00 a.m	19.5091

## Reference

---

- [1] World Energy Council 2014
- [2] BP Energy Outlook Booklet 2013
- [3] WORLD ENERGY OUTLOOK 2013
- [4] <http://www.climatechangedispatch.com/china-s-coal-trends-myth-reality.html>
- [5] Climate change dispatch. <http://www.climatechangedispatch.com/china-s-coal-trends-myth-reality.html>
- [6] Future of electricity attracting investment to build tomorrow's electricity sector report2015 pdf
- [7] [https://en.wikipedia.org/wiki/Energy\\_development](https://en.wikipedia.org/wiki/Energy_development)
- [8] [https://en.wikipedia.org/wiki/Energy\\_policy\\_of\\_India](https://en.wikipedia.org/wiki/Energy_policy_of_India)
- [9] Energy scenario and vision in 2020 in India by P. Garg.
- [10] Energy statistic report of India 2014 pdf.
- [11] energy statistic 2014 India
- [12] Global energy trend BP statistic review.
- [13] <http://www.firstgreen.co/2013/08/all-india-electricity-consumption-sector-wise-end-of-ist-year-of-12th-plan/>.
- [14] <http://www.eia.gov/beta/international/analysis.cfm?iso=IND>
- [15] [https://en.wikipedia.org/wiki/Electricity\\_sector\\_in\\_India](https://en.wikipedia.org/wiki/Electricity_sector_in_India)
- [16] <http://mnre.gov.in/mission-and-vision-2/achievements/>
- [17] United state environmental protection agency
- [18] Environmental Protection Agency. 2012. Inventory of U.S. Greenhouse Gas Emissions and Sinks: 1990-2010
- [19] Energy Information Agency (EIA). 2012. How much of the U.S. carbon dioxide emissions are associated with electricity generation
- [20] Scientists(UCS).2009 Union of Concerned. Clean Power Green Jobs.
- [21] National Renewable Energy Laboratory (NREL). 2012. Renewable Electricity Futures Study. Volume 1, pg. 210.
- [22] Machol, Rizk. 2013. Economic value of U.S. fossil fuel electricity health impacts. Environment International 52 75–80.



- 
- [23] [http://www.ucsusa.org/clean\\_energy/our-energy-choices/renewable-energy/public-benefits-of-renewable.html](http://www.ucsusa.org/clean_energy/our-energy-choices/renewable-energy/public-benefits-of-renewable.html)
- [24] SEIA.2012. Solar market inside report 2012.Q3
- [25] UCS.2009.clean power green job. Consumer saving
- [26] UCS.2011. A Risky Proposition: The financial hazards of new investments in coal plants.
- [27] Clean power green job 25 res pdf
- [28] Unger, David J. 2012. Are renewable stormproof Hurricane Sandy tests solar, wind. The Christian Science Monitor. November 19.
- [29] <http://fs-unep-centre.org/publications/global-trends-renewable-energy-investment-2015>
- [30] [https://en.wikipedia.org/wiki/Renewable\\_energy\\_in\\_India#Waste\\_to\\_energy](https://en.wikipedia.org/wiki/Renewable_energy_in_India#Waste_to_energy)
- [31] Global trend in renewable energy investment 2015 pdf
- [32] [https://en.wikipedia.org/wiki/Renewable\\_energy\\_in\\_developing\\_countries](https://en.wikipedia.org/wiki/Renewable_energy_in_developing_countries)
- [33] Schmalensee R, The future of solar energy: A personal assessment, 52, 2015, S142-S148
- [34] UNEP, solar electricity fact sheet
- [35] U.S department of energy solar energy roadmap
- [36] Doll .J, Henning .H-M, solar system for heating and cooling of bulding, 30, 2012, 633-653
- [37] Da-Wen Sun, Thermodynamic design data and optimum design maps for refrigeration system, 17, 1996, 211-221
- [38] DA-WEN SUN, comparison of the performance of NH<sub>3</sub>-H<sub>2</sub>O, NH<sub>3</sub>-LiNO<sub>3</sub>, NH<sub>3</sub>-NaSCN absorption refrigeration system, 39, 1996, pp.357-368.
- [39] S.A. Kalogirou, Solar thermal collectors and application, 30, 2004, pp. 231-295
- [40] M.A. Sabiha , R. Saidur, S. Mekhilef , O. Mahian, Progress and latest developments of evacuated tube solar collectors, 51, 2015, pp. 1038-1054
- [41] Mummer Ozgoren, Mehemet Bilgili, Osman Babayigit, Hourly performance prediction of ammonia-water solar absorption refrigeration, 40, 2012, pp.80-90
- [42] Mazzei S.M, Mussati C.M, Mussati F.S. NLP model-based optimal design of LiBr-H<sub>2</sub>O absorption refrigeration system. International Journal of Refrigeration 2014;38: 58-70
- [43] Ketfi O, Merzouk M, Merzouk K .N, Metenani .El. S. performance of single effect solar absorption cooling system (LiBr-H<sub>2</sub>O). Energy Procedia 2015; 74: 130-138
- [44] Chougui Mohamed Lamine, Zid Said. Energy analysis of single effect absorption chiller (LiBr/H<sub>2</sub>O) in an industrial manufacturing of detergent. Energy Procedia 2014;50: 105-112

- [45] Karno A, Ajib S. Thermodynamic analysis of an absorption refrigeration machine with new working fluid for solar application. *Heat Mass Transfer* 2008;45: 61-70
- [46] Sun DW. Comparison of the performance of NH<sub>3</sub>-H<sub>2</sub>O, NH<sub>3</sub>-LiNO<sub>3</sub> and NH<sub>3</sub>-NaSCN absorption refrigeration system. *Energy Converse* 1998; 39(5/6): 357-68
- [47] Abdulateef JM, Sopian K, Alghoul MA, Sulaiman MY, Zaharim A, Ahmad I. Solar absorption refrigeration system using new working fluid pair. *Int J Energy* 2007; 1(3): 82-87
- [48] Kaynakil O, Kilic M. Theoretical study on the effect of operating condition on performance of absorption refrigeration system. *Energy Converse Manage* 2007;48: 599-607
- [49] M.I. Karamangil, S. Coskun, O. Kayanakil, N. Yamankaradeniz. A simulation study of performance evaluation of single-stage absorption refrigeration system using conventional working fluids and alternative. *Renewable and sustainable Energy Reviews* 2010; 14: 1969-1978
- [50] Weihua Cai, Mihir Sen, Samuel Paolucci. Dynamic simulation of an ammonia-water absorption refrigeration system.
- [51] Vaibhav Jain, S.S. Kachhwaha, Gulshan Sachdeva. Thermodynamic performance analysis of a vapor compression-absorption Cascaded Refrigeration system. *Energy Conversion and Management* 2013;75: 685-700
- [52] A. Saleh, M. Mosa, optimization study of single –effect water-lithium bromide absorption refrigeration system powered by flat plate collector in a hot region, 87,2014, pp.29-36
- [53] Ibrahim Atmaca, Abdulvahap Yigit, simulation of solar-powered absorption cooling system,28,2003, pp.1277-1293
- [54] Syed A.M.Said, Maged A.I. El-shaarawi, Muhammad U. Siddiqui. Alternative design for a 24-h operating solar-powered absorption refrigeration technology.
- [55] M.Hammad, Y.Zurighat. performance of a second generation solar cooling unit, 62, 1998, pp.79-84
- [56] N.K. Ghaddar, M.Shihab, F. Bdeir. Modelling and simulation solar absorption system performance in Beriut,10,1997,pp.539-558
- [57] F.Assilzadeh, S.A. Kalogirou, Y. Ali, K.Sopian. Simulation and optimisation of LiBr solar absorption cooling system with evacuated tube collector,30,2005,pp.1143-1159.
- [58] A.Iranmanesh , M.A.Mehrabian, Optimization of a lithium bromide–water solar absorption cooling system with evacuated tube collectors using the genetic algorithm,87,2014,pp.427-435

- [59] Christine Weber , Michael Berger , Florian Mehling a , Alexander Heinrich a , Solar cooling with water-ammonia absorption chillers and concentrating solar collector e Operational experience,39, 2014,pp.57-76
- [60] Ali Al-Alili , Yunho Hwang. Reinhard Radermacher Review of solar thermal air conditioning Technologies,39,2014,pp.4-22
- [61] R.Z. Wang , Z.Y. Xu, Q.W. Pan, S. Du, Z.Z. Xia. Solar driven air conditioning and refrigeration systems corresponding to various heating source temperatures,169, 2016,pp. 846-856
- [62] Ali Shirazi , Sergio Pintaldi , Stephen D. White , Graham L. Morrison , Gary Rosengarten , Robert A. Taylor. Solar-assisted absorption air-conditioning systems in buildings: Control strategies and operational modes, 92,2016,pp.246-260.
- [63] Elisa Viñas , Roberto Best , Sergio Lugo. Simulation of solar air conditioning systems in coastal zones of Mexico, 97, 2016, pp. 28-38
- [64] F.J. Cabrera , A.Fernández-García , R.M.P.Silva, M.Pérez-García. Use of parabolic trough solar collectors for solar refrigeration and air-conditioning applications,20, 2013, pp.103-118
- [65] Safwan Kanana, Jonathan Dewsburya, Gregory F. Lane-Serffa. Simulation of Solar Air-Conditioning System with Salinity Gradient Solar Pond, 79, 2015, pp. 746-751
- [66] A.A. Al-Ugla, M.A.I. El-Shaarawi, S.A.M. Said. Alternative designs for a 24-hours operating solarpowered LiBrewater absorption air-conditioning technology,53, 2015, pp. 90-100
- [67] Thermo physical properties of {NH<sub>3</sub>+H<sub>2</sub>O} solution for the industrial design of absorption refrigeration equipment. M.Conde Engineering 2004
- [68] Wagner.W, Kruse.A. Properties of water and steam-The industrial standard IAPWS-IF97 for the thermodynamic properties and supplementary equations for other properties, Spinger-verlag, Berlin
- [69] Zinner, K. 1934. Warmetönung beim Mischen von Ammoniak and wasser in Abhagigkeit von Zusammensetzung and Temperature, Zeith, for die gesamte kalte-Industries,41(2),21-29
- [70] S P Sukhatme. Solar Energy. Principles of thermal collection and storage.
- [71] I. Atmaca, Abdulvahap Yigit. Simulation of solar- powered absorption cooling system. Renewable energy 2003;28: 1277-1293
- [72] NREL (National Renewable Energy Laboratory)